COMPUTER SIMULATION OF COPPER AND TUNGSTEN CRYSTAL DYNAMICS WITH VACANCIES AND INTERSTITIALS

Gary Lee Vine

United States
Naval Postgraduate School

THESIS

COMPUTER SIMULATION OF COPPER AND TUNGSTEN CRYSTAL DYNAMICS WITH VACANCIES AND INTERSTITIALS

by

Gary Lee Vine

Thesis Advisor: Don E. Harrison, Jr.

June 1971

Computer Simulation of Copper and Tungsten Crystal Dynamics With Vacancies and Interstitials

by

Gary Lee Vine
Ensign, United States Navy
B.S., United States Naval Academy, 1970

Submitted in partial fulfillment of the
requirements for the degree of

MASTER OF SCIENCE IN PHYSICS

from the

NAVAL POSTGRADUATE SCHOOL
June 1971

ABSTRACT

The effects of point defect implantation in copper and tungsten crystal lattice have been studied by computer simulation techniques. Vacancies, interstitials, and replacement impurities have been created in the first five layers of the free (100) surface of these crystals. The subsequent binding energies of these defects in tungsten were compared with experimental temperature dependent desorbtion peaks, corresponding to binding energies of neon defects in a tungsten crystal. Interstitial and replacement impurity positions in the first three to five layers were found that seem to correspond to the experimental data. Significant results were also obtained which were associated with general surface effects, especially crowdion migration.

TABLE OF CONTENTS

LIST OF FIGURES

ACKNOWLEDGEMENT

I am deeply indebted to Professor Don E. Harrison, Jr., for the time, effort, and resources which he has contributed to this project, as well as the interest and encouragement he has offered. I am indebted to the many people in the NPS Computer Facility for their help, personal attention, and valuable computer time. I am especially indebted to my wife for the many hours of effort and encouragement which she has contributed to this project.

I. INTRODUCTION

Extensive research has taken place in the last decade in the area of computer simulation of radiation damage in crystal lattices. Two major areas of simulation have been defined. "Dynamic simulation" suggests the firing of an atom or ion against a crystal and the observation of the resulting many-body collisions. Examples include sputtering simulation [1,2,3], in which atoms are ejected from the surface of an ion-bombarded crystal; and channeling simulation [4], in which ions are fired down open channels in non-close-packed structures such as body-centered cubic and diamond lattices. "Static simulation", on the other hand, is concerned with equilibrium positions and energies for point defects in crystals [5,6,7]. This latter area was the concern of this research. Specifically, this simulation attempted to correlate equilibrium potential energies of point defects with experimentally determined binding energies of point defects in Tungsten [8,9].

A. HISTORICAL BACKGROUND

1. The Problem

Historically, all crystal dynamics computer simulation has been based on the assumption that the complicated many-body problem can be reduced to many two-body problems. This assumption has repeatedly been shown to be a valid one when employed incrementally. Incremental calculations are necessary since a complete solution in closed form is impossible. Small time increments Δt approximated the true time differential dt of the impossible closed form

solution. Specifically, the desired type, size, and orientation of crystal lattice is stored in the computer, appropriate interatomic potentials are chosen, and all mutual forces between atoms are calculated, based on the analytic potential functions. Point defects are introduced, and each atom is then allowed to move incrementally, based on these forces and Newtonian Mechanics [5]. Through proper choice of time increment duration, damping of forces and velocities in each time increment, and sufficient repetition of the procedure, realistic results are obtained.

2. The Pioneers and Their Contributions

Pioneering work in this field began in the early 1960's at the Brookhaven National Laboratory. Gibson, Goland, Milgram and Vineyard (GGMV) [5] published the results of extensive work in both static and dynamic simulation. In static simulation they determined equilibrium positions for interstitials and associated potential energies of formation. In dynamic simulation they investigated momentum propagation directions of energetic knock-on atoms (focusing), collision chains, and related topics. They used a central-difference method to obtain velocities and positions from calculated forces. All work was done with copper, and results were correlated with experimental data. Johnson and Brown (JB) [6] did extensive work in static simulation, again with copper. They established that only one stable position exists for a single face-centered cubic (FCC) self-interstitial: the ⟨100⟩ split interstitial. Johnson [10] later published further work in this area, with formation and activation energies for various point defects. Enginsoy, Vineyard, and Englert (EVE) [7] and Johnson [11]

repeated most of the earlier calculations in GGMV and Johnson for the body-centered cubic (BCC) case, based on α iron. They, too, established the existence of only one stable interstitial position, a $\langle 110 \rangle$ split interstitial.

Girifalco and Weizer (GF) [12] calculated Morse Potential

$$\Phi_{ij} = D[\exp\{-2\alpha(r_{ij}-r_o)\} - 2\exp\{-\alpha(r_{ij}-r_o)\}]$$

parameters for various metals, based on experimental values for the energy of vaporization, the lattice constant, and compressibility. Resulting elastic constants and equations of state agreed satisfactorily with experiment. Girifalco and Weizer [13] later published results of using these Morse parameters in simulating vacancy relaxation dynamics. Anderman [14] used GW's technique of calculating Morse parameters, but instead of summing over an entire crystal, (GW calculated out to the 150th nearest neighbor) Anderman found parameters as a result of summing out to second, third, and fourth nearest neighbors, for use in short-range approximations.

Harrison [1,2,3] has investigated sputtering phenomenon and other surface effects with a modified Brookhaven model, the most significant change being the use of an average force method [15] instead of the central difference method in integrating the equations of motion. (See Appendix C.) He has also calculated repulsive potentials of the Born-Mayer type ($V_{ij} = \exp(A+Br_{ij})$) for many combinations of atoms and ions based on secondary electron emission, and Hartree-Fock atomic electron distributions [16].

3. The Potential Function Problem

The most difficult problem encountered by computer simulation has been the proper choice of the potential function. No simple analytic expression, based on either theory or experimental data, has ever been found that completely describes crystal dynamics [17], although many analytic expressions are partially correct. The problem has been three-fold: First, present analytic expressions have narrow regions of validity, i.e., some correctly describe atomic behavior at equilibrium distances, but fail at shorter or greater distances. Second, some analytic expressions are limited because they only apply to interactions between identical atoms. Third, the assumed functions have spherical symmetry, and are technically limited to interactions between closed shell atoms or ions [18]. Although our assumption of a spherically symmetric potential in crystals is only approximately correct, it is nevertheless a very good approximation for FCC structures, and a reasonably good approximation for BCC structures. It is grossly in error when applied to diamond structures.

The atomic potential, with the familiar potential well, sharply repulsive wall and gently attractive tail, varies greatly between different pairs of atoms. Since theory can give only approximate parameters for this complete potential function, experimental data have been used extensively in the formulation of potentials. Other avenues have been opened by computer simulation. Since potential well depths are typically on the order of a few eV, the characteristics of the well can be ignored in high energy dynamic simulation. Low energy dynamic simulation, and even static

simulation, have also been based upon this approximation with useful results. Historically this is how crystal simulation began. GGMV [5] employed a purely repulsive potential of the Born-Mayer (BM) type and applied external forces on all crystal boundaries to hold the crystal together. JB [6] used basically the same technique. For improved equilibrium studies a potential with a well was necessary so GW [12,13] used a Morse potential in their simulation. The Morse function, however, fails at strongly repulsive distances. To satisfy the need for a more versatile potential, capable of handling both high energy and near-equilibrium dynamics, composite potentials were developed, which resemble BM or Bohr

$$(V_{ij} = \frac{r'}{r_{ij}} \exp(A+Br_{ij}))$$

functions at short separations, and Morse functions at equilibrium and greater separations. Specifically, EVE [7] combined a screened Coulomb or Bohr potential, a BM potential, and a Morse potential, in the higher repulsive, lower repulsive, and attractive regions, respectively, of the atomic potential.
Johnson [10,11] in his later papers, used three cubic equations to approximate the true potential. Anderman [14] and Harrison [1,2,3,4] have used the BM repulsive term together with a Morse well and attractive tail, smoothly fit together by a cubic equation in the region near their intersection.

4. The Point Defect Problem

All early simulation was done with homogeneous systems: All atoms were exactly the same, limiting high energy dynamic simulation to bombardment by atoms identical to the lattice atoms,

and static simulation to consideration of only the vacancy and self-interstitial cases. This limitation was forced by the potential functions, because parameters for the Morse function were based on experimental data for homogeneous media [12]. The methods used could not yield parameters for different-atom pairs. BM parameters, however, are obtainable for different-atom pairs, by methods such as the Hartree-Fock method [16] mentioned previously.

In spite of these limitations, dynamic computer simulation of bombardment by foreign atoms, or static simulation of foreign interstitials, can be done by two alternate methods. First, Harrison [4] has neglected the attractive interactions and has done foreign particle dynamics using repulsion only. Alternately, Johnson [11] has derived a cubic equation for a complete potential with a potential well, based on limited experimental data on carbon defects in iron. However, experimental substantiation for a foreign-particle potential well is much more difficult than for an identical atom potential well.

B. THE EXPERIMENT

The experimental data which this simulation proposed to explain, were published by Kornelsen and Sinka (KS) [8]. They have bombarded a clean (100) tungsten surface with Ne^+, Ar^+, Kr^+, and Xe^+, in the energy range of 40 eV to 5 keV. The subsequent "damaged" crystal was heated at a constant rate, and gas desorbtion rates were measured. Instead of a constant desorbtion of ions, various distinct peaks were found, categorized into two basic types: a

single large peak at $1800^{\circ}K$, the same for all four ions; and four or five smaller peaks in the $400^{\circ}K$ to $1650^{\circ}K$ range, which were not in the same position for all four ions. These latter peaks were postulated to correspond to binding energies of various point defects in the first few layers of the tungsten crystal. (See Figure 4.)

This simulation used Harrison's assumption of a repulsive potential only, for interactions between a foreign point defect and other atoms in the lattice. When investigating neon defects in tungsten, all tungsten lattice interactions were based on composite Morse and repulsive Born-Meyer potentials, and all neon-tungsten (Ne-W) interactions were based on a purely repulsive BM potential.

II. OBJECTIVE

The long-range objective of this simulation was to correlate simulated and experimental binding energies of neon point defects in tungsten. Since the assumption that all Ne-W interactions are purely repulsive was not realistic, the degree to which subsequent simulation results are valid must be based on a known standard. If the simulated binding energies are not correct, a valid correction factor can be applied, if derivable from the known standard. One standard which proved to yield this information was the tungsten-tungsten (W-W) interaction. A tungsten point defect could be treated as an atom of the lattice, and given an interatomic potential identical to all other lattice atoms, the composite Morse and BM potential. This was Method 1. A tungsten defect could also be treated as foreign, and allowed to interact with other lattice atoms with a repulsive potential only (Method 2). If a specific tungsten point defect is treated by both of these methods, an empirical relationship between the repulsive potential assumption and the "true" potential for W-W interactions is obtained.

The objectives of this research were fourfold:

1. Demonstrate that the two methods of treating tungsten point defect in a tungsten lattice yield basically the same physical results, and agree with published results [7,11] concerning split interstitial positions.
2. Develop a general empirical relationship between the binding energies derived by the two methods.

3. Obtain values for binding energies of neon defects in all possible positions in a tungsten surface. Transform these values to more realistic ones using the empirical relationship derived in 2.

4. Compare these results with KS's experimental data.

III. THE MODEL

A. THE CRYSTAL

The model used in this research is the Gay-Harrison [19] model, with modifications by Levy [20], Johnson [21], Effron [22], and Moore [23]. Abbreviations in brackets refer to computer program names for the variable in question.

Both copper and tungsten crystals were simulated. Copper was simulated only to provide an interface between this research and published simulation results. Copper forms a face-centered cubic crystal with an experimentally determined lattice constant, (LC) or cube edge distance of 3.615Å. The lattice unit (LU), defined as ½LC, is 1.8075Å; and the nearest neighbor distance, as in all FCC structures, is $\sqrt{2}$LU. Tungsten forms a body-centered cubic crystal, with a LC of 3.16Å, a LU of 1.58Å, and a nearest neighbor distance, peculiar to all BCC structures, of $\sqrt{3}$LU. All distances in the program are measured in LU. The program could construct (100), (110), and (111) orientations of face-centered and body-centered cubic structures. The copper crystal size was 8 x 8 x 8, and contained 256 atoms for the (100) orientation.

The major portion of the simulation was done on the (100) orientation of tungsten, corresponding to KS's experimental work. This tungsten crystal size for Neon point defects was 10 x 10 x 10, and contained 250 atoms. Some W-W simulation was done on a 14 x 14 x 14 crystal; the reasons are explained in RESULTS. The bottom two layers of the lattice were not allowed to move, although they had potential energy, and exerted force on all atoms

in the crystal. The other eight layers were completely free to move, and were included in the dynamic calculations of each time-step.

The surface layer (Y = 0) and the second layer (Y = 1) were moved forward, simulating actual surface relaxation in the crystal. This relaxation was calculated by Moore [24] using simulation techniques, and tested against previous results by Burton and Jura [25]. Definitions and use of mobile layers, relaxation, etc., were analagous in the copper model, as were all other aspects of the model to be described in this chapter.

B. THE POTENTIALS

1. The W-W Composite Potential

The attractive potential used was the Morse potential, with tungsten parameters calculated by GW [12]. The interaction energy ϕ_{ij}, of a pair of particles i and j is:

$$\phi_{ij} = D[\exp\{-2\alpha(r_{ij}-r_o)\} - 2\exp\{-\alpha(r_{ij}-r_o)\}] \qquad (1)$$

where D [DCON] is the dissociation energy of the pair, r_o[RE] is the equilibrium separation, r_{ij}[DIST] is the actual separation, and α [ALPHA] is a constant.

The repulsive potential is of the BM type, with Harrison's Hartree-Fock parameters. The interaction energy V_{ij}, is

$$V_{ij} = \exp(A+Br_{ij}) \qquad (2)$$

where B [EXB] is always negative, A [EXA] is always positive, and r_{ij} [DIST] is the actual separation. The constants [EXA] and [EXB] are peculiar to the W-W interaction.

The ranges of the W-W composite potentials were as follows: the BM repulsive potential operated from 0 to 1.5Å; and the Morse potential from 2Å [ROEB] to 5.38Å [ROEC]. In LU, the dimension in which all calculations were done, these constants were .9494, 1.2658, and 3.4000 LU. [ROEC] was chosen to include interactions out to the fourth nearest neighbor (NN4) at $\sqrt{11}$ LU = 3.317 LU but not NN5 interactions, at $\sqrt{12}$ LU = 3.464 LU. Note, however, that slight displacements of NN5's might allow their inclusion in potential and force calculations. The gap between 1.5Å and 2Å was filled with a cubic function, which matched to the other potentials and slopes at [ROEA] and [ROEB].

2. Purely Repulsive Potentials

For foreign point defect interactions, i.e., Ne-W, or W-W Method 2, a repulsive potential only was used. The potential was again a BM, with the constants labeled [PEXA] and [PEXB]. For the W-W, Method 2 interaction, [PEXA] = [EXA] and [PEXB] = [EXB]. Ranges for foreign point defect interactions, however, were different, and the potential itself was modified at the cutoff point. Whereas the BM part of the composite potential extended out to about .95 LU, the modified BM potential used for foreign defects was allowed to extend to $\sqrt{3}$ LU, corresponding to the NN1 distance [ROE]. Cutting the potential off at [ROE] left a step of about .05 eV for Ne-W (.2 eV for W-W) at the NN1 equilibrium position. Since neither discontinuities nor repulsive potentials were desired at this equilibrium position, we "eroded" [15] the potential by subtracting V([ROE]), or about .05 eV from $V(r_{ij})$ for r_{ij} < [ROE]. Calculated forces, based on these eroded potentials must be modified also, but for a different reason. It is possible

to conceive of a case where an atom is further away from the defect than [ROE] at the beginning of a timestep, but closer than [ROE] at the end. The force has essentially "turned on" in the middle of the timestep. The modification gives such an atom a force which is less than the final force by approximately a factor proportional to the ratio of distance traveled outside [ROE] to the total distance traveled during the timestep [15]. (See Appendix B.)

C. THE TIMESTEP

Motion caused by these forces must be found by an approximate numerical method of time integration. As in previous work with this model, the average force method [15] was used. In this method, all mutual forces were calculated in subroutine STEP. Based on these forces, new temporary velocities and positions were found. Forces were again calculated, based on the temporary positions. The final positions were then calculated from the average of these two force determinations. All velocities were then either zeroed or halved as a damping method. This constituted one timestep.

For this average force method to work properly, the Δt[DT] which approximates dt in the integration must be kept small. Too small a value for [DT], however, would result in excessive computer time. The choice of [DT] was also complicated by the fact that [DT] must be kept much smaller earlier in the program, when velocities, forces, and energies are large, but can be allowed to grow larger as the simulation approaches equilibrium. For this reason, at the end of each timestep, a new [DT] was calculated

for use in the next timestep. The parameter chosen to control [DT] was [DTI], the distance, measured in LU, which the most energetic atom was allowed to move before starting a new timestep. [DTI] has varied between .001 and .02, depending on such conditions as original position of the point defect, relative masses of atoms, etc. In general, [DTI] must be kept very small when high velocities are expected, and can be increased when all motion is expected to be "sluggish". In actual practice [DT] and [DTI] are related to both the velocity of each particle and the force on each particle. To insure that no particle traveled more than [DTI] we ensured that [DT] was small enough so that neither the velocity of the most energetic atom nor the force on the most stressed atom would result in motion greater than [DTI]. (See Appendix C.)

D. FOREIGN INTERSTITIALS

1. Unequal Mass Implications

Many changes in the program were necessary when a foreign defect was included in the lattice. These changes were especially necessary when the defect was much lighter than the lattice atoms; i.e., neon in a tungsten lattice. First, in the average force calculations, a separate section had to be added for the calculations for the primary, or "bullet", based on the bullet mass [BMAS]. Second, the potential energy between two unequal mass atoms was split in proportion to their reduced masses (See Appendix D). Third, the section that determined the new timestep duration was originally based on the lattice atom mass. Since the light interstitial is usually the most energetic or most stressed

atom, very erratic behavior was observed until the timestep duration calculations were revised to handle two different masses (see Appendix C). Finally, a significant mass difference between defect and lattice atom required a reduction in [DTI]. For the neon-tungsten simulation, a [DTI] of .5% was used.

2. Ionization State and Repulsive Potentials

The major portion of the Ne-W work was done with the assumption that tungsten was in a +6 state, and neon was neutral in the lattice. Experimentally KS fired neon in a +1 state into tungsten, but once emplanted, the ionization of neon was unknown. All combinations of W^{o}, W^{+1} and W^{+6} with Ne^{o} and N^{+1} were subjected to Hartree-Fock analysis. (See Figure 5.) Only Ne^{o}-W^{+6} interacted in an approximately exponential manner and could therefore possess realistic BM parameters. Attempts to linearize Ne^{o}-W^{+1} and Ne^{o}-W^{o} were made, and subsequent BM parameters were determined. The results of such changes did not significantly influence the results of this investigation.

E. RUNNING TIME

The following factors effected the problem running time: range of potential, size of crystal, depth of mobile layers, and degree of damping. First, the range of the potential was picked to include at least NN4 interactions. The range used for the tungsten simulation was 3.4 LU, which includes interactions out to NN4. The error made by neglecting NN5 interactions was only 3% in the binding energy of an interstitial, but the omission of NN5 interactions cut running time almost 10%. Second, the size of crystal and depth of mobile layers were picked as small as possible, for

reduced running time, but were at least large enough to completely contain the potential range. Third, the half velocity method of damping was used whenever possible. In general, when velocities were zeroed at the end of each timestep, a timestep took about ten seconds, and equilibrium was reached in about 300 timesteps. When velocities were halved, each timestep again took about ten seconds, but equilibrium was reached in about 150 timesteps.

It was originally expected that increasing [DTI] would decrease running time. Most W-W simulation was done with [DTI] = 2%; i.e., the most energetic or stressed atom could travel .02 LU before the damping of velocities and the starting of a new timestep. When [DTI] was increased, the atoms moved more erratically toward equilibrium, and vibrated there, but did not achieve equilibrium significantly sooner. (See Figure 6.)

F. SUMMARY

In summary, the steps of the program are outlined:

1. Variables are initialized, constants established, and input data read in.
2. Scaling factors and time saving multipliers are calculated.
3. Morse and BM potential functions are calculated based on input data. Subsequent forces, based on derivatives of these functions are calculated. Potential erosion and force modifications are performed.
4. Potential cutoff's [ROEA], [ROEB], [ROEC] are established and the smooth fitting cubic equation is placed in the gap.
5. The desired crystal type, size, and orientation is built, and the point defect positioned (see Appendix A).

6. Mutual potential energies of all atoms in the crystal are calculated. Local potential energy is calculated. (See Appendix D.)

7. All initial positions and potential energies are printed, along with total potential and total kinetic energy, local potential energy, and the change in local potential energy.

8. The first timestep is started, with an arbitrary running time of 10^{-14} sec. Velocities and positions are calculated by the average force method, and the maximum velocity [EMAX] and maximum force [FMAX] are found.

9. A new [DT], based on [EMAX], [FMAX], and [DTI] is calculated for use in the next timestep. (See Appendix C.)

10. All velocities are zeroed or halved as an energy damping method, and the process (8. to 10.) is repeated.

11. At selected timesteps, all changes in position ([DX], [DY], [DZ]), velocities ([VX], [VY], [VX]), and kinetic, potential, and total energies [PKE], [PPE], [PTE] for each atom in the crystal are printed.

12. The program is ended after a pre-selected timestep, with a final printout of position and potential energy of each atom, as in Step 7.

IV. RESULTS

KS's experimental data indicated that four or five interstitial positions in the first few layers of a tungsten lattice could be found that would result in different binding energies. It was soon found that many parameters in the program could effect the results, and so a systematic attempt to isolate the effects of each individual parameter was undertaken.

A. THE CRYSTAL

As explained in Appendix A, the Y = 0 plane was the crystal surface; the Y = 1 plane was the first layer beneath the surface, etc. Each atom in each layer was then designated by appropriate x and z coordinates. This construction was independent of type of lattice; i.e., the surface layer in either BCC (100) or FCC (100) was Y = 0, etc. An interstitial that escaped the lattice normal to the surface travelled in a ⟨010⟩ direction, and an ion that escaped normal to a side travelled in either a ⟨100⟩ or ⟨001⟩ direction.

The dimensions of the lattice had a great bearing on the results. In general, the larger the crystal, the more realistic the results, but increased computer time prevented the use of a size bigger than absolutely necessary. All point defects were placed as close to the center of each plane as possible, and the x and z dimensions of the lattice [IX] and [IZ] were chosen to completely enclose a circle of radius [ROEC] from the point defect. In this way any point defect in the center of the lattice would not feel

the effect of the sides of the lattice, especially unequal numbers of atoms in all directions. In the y direction, the lattice was again built deep enough to completely contain the radius of the potential of a point defect placed at the center of the lattice. To simulate the effect of an infinitely deep lattice, the bottom two layers of the crystal were held immobile, but still allowed to interact with all mobile atoms above them. The tungsten crystal size used most often was a 10 x 10 x 10 cube with the bottom 10 x 2 x 10 volume held rigid.

Often erratic behavior in the simulation could be eliminated by simply increasing the crystal size. This was especially true for the problem of crowdion migration.

B. CROWDION MIGRATION

Crowdion migration is a chain reaction of single lattice site jumps initiated by interstitial implantation. If the chain reaction ends by pushing the surplus atom into an already existing vacancy, the interstitial-vacancy pair is called a Frenkel pair. A Frenkel pair can also be created dynamically by moving an atom from its lattice site to a nearby interstitial position, from where it can cause migration back to the vacancy. If the migration cannot find a vacancy, and travels all the way to the surface, the surplus atom forms a "stub". Normally, migration is always in a closed packed direction; i.e., in the $\langle 111 \rangle$ direction in BCC. It was discovered, however, that this rule was modified near a surface, since an imbalance of forces in the direction normal to the surface automatically pushed a crowdion in that normal direction into a stub position. In the tungsten

lattice, for instance, a tungsten interstitial that did not initiate crowdion migration would reach equilibrium in a ⟨110⟩ split interstitial position, as previously found by EVE [7]. A tungsten interstitial that did initiate crowdion migration would sometimes migrate in a ⟨111⟩ direction because of closed-packedness, or sometimes in a ⟨100⟩ direction if implanted near a (100) surface. Crowdion migration was never found in a ⟨110⟩ direction, since this is the least closed-packed of these three directions. (Hence the tendency toward split-interstitials in this direction).

Crowdion migration was a very common process near a lattice surface. It was found, however, that varying the choice of atoms, the range of the potential, and the rate of energy damping could enhance or reduce the tendency toward crowdion migration. Also, already mentioned was the fact that increased crystal size re-reduced crowdion migration. Particular attention was paid to the proper choice of values for these parameters, in order to correctly determine whether or not crowdion migration actually existed. This question of crowdion migration was especially critical in this simulation, since the binding energy of a particular atom is a direct function of the nearness of its neighbors. An atom in a split interstitial position feels a more repulsive potential than an interstitial that has initiated crowdion migration and 'stolen' a lattice site and has thus reformed the original perfect lattice with every atom in a normal lattice site.

1. <u>Choice of Atom</u>

Some elements tended to initiate crowdion migration more than others. This applied to both choice of lattice atom, and

choice of interstitial atom. For instance, crowdion migration was much more common in tungsten than in copper. This was due to both the size of the tungsten atom and the nature of the crystal. Also it was found that different element point defects in the same lattice produced varying degrees of crowdion migration. A neon interstitial is so small and light that it never initiated crowdion migration, even when only one layer separated it from the surface. An argon interstitial initiated crowdion migration at the surface, but not deeper in the lattice. A tungsten interstitial always initiated crowdion migration, unless placed at the center of a huge 14 x 14 x 14 tungsten lattice. This is an example of increasing crystal size to prevent crowdion migration. In general it can be stated: the more massive the interstitial, the more probable crowdion migration.

2. Range of Potential

In surface simulation, the range of the potential was a critical factor, since it determined whether or not an atom could "see" the surface. Because copper has been the standard element for lattice simulations, many versions of a copper potential with various ranges, have been determined. As mentioned previously, GW [12] calculated a Morse potential for copper that effectively had an infinite range (150th nearest neighbor). If this potential is truncated at very close ranges, i.e., NN1 or NN2, the potential is seriously underestimated. This under estimate rapidly diminishes as the truncation range increases. Since GW parameters for the Morse potential could not be used for NN2 interactions, Anderman [14] calculated parameters for a Morse copper potential that would approximate GW's results in simulations truncated after

NN2. He did this by deepening and broadening the well. Although Anderman parameters and GW parameters led to very similar results in an infinite lattice, they led to quite different results in this simulation. In general, if the range of a point defect potential function overlapped a surface, crowdion migration would take place toward that surface, because of an imbalance of forces in the normal direction. The effect was a little more complex than this because of surface relaxation: if the range of the point defect potential function overlapped a relaxed surface layer, the slight force imbalance would again result in crowdion migration. According to GGMV, "the machine calculation showed that this atom rapidly moved...in a direction determined by minor asymmetries in the starting conditions..."[1]. In this copper simulation, an interstitial placed in the forth layer with a GW potential range of 3.1 LU (NN4) caused complete crowdion migration, resulting in a copper stub on the surface. An identical run with Anderman parameters for an NN2 potential to a range of 2.4 LU resulted in a ⟨100⟩ split interstitial with minor, damped migration to the surface. Instead of a stub copper atom as before, four copper atoms in the surface layer bulged about .4 LU.

Another example of a short range potential which demonstrated this lack of ability to initiate crowdion migration was the repulsive foreign defect potential, with a range of $\sqrt{3}$ LU. In copper, this potential quickly led to split interstitial positions and no crowdion migration for all copper interstitials

---

[1]Gibson, J.B., Goland, A.N., Milgram, M., and Vineyard, E.H., "Dynamics of Radiation Damage,"The Physical Review, V. 120, No. 4, p 1237, Nov 15, 1960.

except those placed in the first two layers. In tungsten, even this short range potential could not retard crowdion migration in the 10 x 10 x 10 lattice. Only in the center of a 14 x 14 x 14 was a tungsten split interstitial stable. This stability applied only to the short range repulsive potential: a repeat run using the standard composite potential with a range of 3.4 LU initiated crowdion migration. This increased range enabled the interstitial to find minor asymmetries in even a 14 x 14 x 14 lattice.

3. Energy Damping

Energy damping was accomplished in this simulation by reducing each atom's velocity at the end of each timestep. Two methods were used: at first, each velocity component of every atom in the crystal was zeroed at the end of each timestep. Later, the halving of each velocity component at the end of each timestep was employed to save computer time. In a tungsten lattice the results of both methods were the same; all final positions and binding energies were identical. Neither method prevented crowdion migration. In copper, these two methods led to slightly different results. Although the final position and binding energy of an interstitial was almost identical, and although crowdion migration was initiated in both cases (GW's parameters and a 3.1 LU range were used), the zeroed velocity method had damped the migration significantly by the time it reached the surface, whereas the halved velocity method caused a complete, undamped migration to the surface.

C. INTERSTITIAL IMPLANTATION

All interstitials were placed in the obvious holes in a hard sphere, close-packed lattice model. (See Figure 7.) Every "hole" in the tungsten lattice had exactly the same geometry; i.e., two neighbors 1 LU away; four neighbors 2 LU away, four neighbors 3 LU away, etc. The only factors which differentiated between these identical holes and thus led to different binding energies were: layer number, or lattice depth, and open channel direction. An interstitial in the third layer was more tightly bound than one in layer two, etc. Also, an atom in a given layer could be placed in two types of holes: one in which the interstitial was in the BCC ⟨010⟩ open channel direction, in which case the interstitial could "see" the surface; and one in which the interstitial was in the BCC ⟨100⟩ or ⟨001⟩ open channel, in which the interstitial could not "see" the surface. Note, however, that if an atom could not "see" the surface, then there was no difference between these two positions, since both have two neighbors 1 LU away, four neighbors 2 LU away, etc. Note also that even if these two sites are identical and possess exactly the same binding energies, the difference might still show up in diffusion probababilities: an interstitial in a ⟨010⟩ open channel in the second layer must only move two lattice units to escape the crystal. An interstitial in a ⟨100⟩ or ⟨001⟩ open channel must move 1 LU in either the x or z direction into an open channel, and then 2 LU to escape; i.e., it must move like a knight in chess. This extra step might lead to a different diffusion probability.

D. THE TUNGSTEN LATTICE SELF DEFECT

The tungsten self interstitials and self replacement defects were the chosen standard for this analysis, as explained in the in the OBJECTIVE. The tungsten defects could be treated as lattice atoms and allowed to interact with all other atoms with the composite potential (Method 1); or they could be treated as foreign defects and allowed to interact with only a repulsive potential (Method 2). A total of three different defect positions were simulated: an interstitial in a $\langle 010 \rangle$ open channel (int A), an interstitial in a $\langle 100 \rangle$ or $\langle 001 \rangle$ open channel (int B), and a replacement atom (rep) in a lattice site. (See Figure 7.)

1. Interstitials

As previously mentioned, all tungsten interstitials initiated crowdion migration when treated by method 1. An interstitial treated by method 2 also initiated crowdion migration unless buried in the center of an enlarged 14 x 14 x 14 lattice. Because an interstitial that has pushed its neighbors away has a lower potential than one that has not done so, the numerical values for binding energy of tungsten interstitials could not serve as a true standard for comparison with W-Ne results. Qualitatively, however, much could be learned from the W-W energy levels. First, it was expected that all energy levels of a defect found by Method 1 would be negative at equilibrium. Values for the composite potential can be either negative or positive, but are positive only at very small separations. A negative potential energy means the atom is bound in the crystal. As shown in Figure 1, on the next page, the first two interstitial levels for the W-W reaction, Method 1, were at -3.0 eV and -3.1 eV, corresponding to

FIGURE 1.

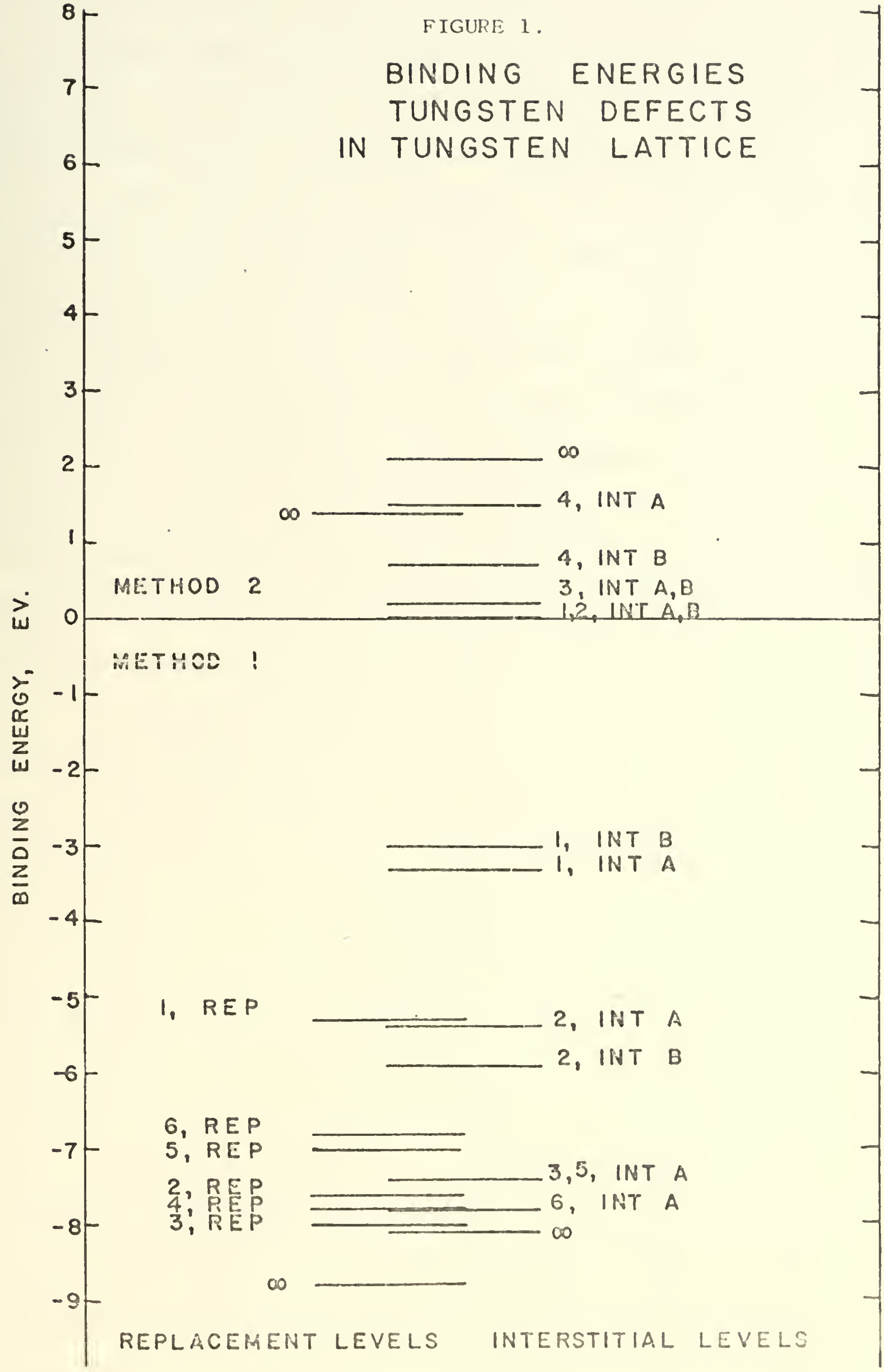
BINDING ENERGIES
TUNGSTEN DEFECTS
IN TUNGSTEN LATTICE
BINDING ENERGY, EV.
8
7
6
5
4
3
2
1
0
-1
-2
-3
-4
-5
-6
-7
-8
-9
METHOD 2
METHOD 1
∞
4, INT A
∞
4, INT B
3, INT A,B
1,2, INT A,B
1, INT B
1, INT A
1, REP
2, INT A
2, INT B
6, REP
5, REP
3,5, INT A
2, REP
4, REP
6, INT A
3, REP
∞
∞
REPLACEMENT LEVELS
INTERSTITIAL LEVELS

the two interstitials in the first layer (int A and int B). The next two levels were at -5.4 eV and -5.9 eV, corresponding to the interstitials in the second layer. Interstitials in the third layer and deeper had binding energies ranging from -7.4 eV to -8.1 eV. The value of -8.1 eV, labeled "∞" was obtained from the interstitial placed in the center of the seventh layer of a 14 x 14 x 14 lattice. Since this value, and all other values for Method 1 binding energies were reached after crowdion migration, they were all expected to be lower than they would be without crowdion migration. The only way the true binding energy of a tungsten interstitial could have been found would have been to find a tungsten crystal size large enough to contain the crowdion migration of a tungsten interstitial with the long-range composite potential. Compute running time made this impossible.

Also shown in Figure 1 are the binding energies for the Method 2 W-W interstitials. Note, first, that they were all positive. This was again expected, since the potential equation for Method 2 is positive over all space. Note, second, that the binding energies for interstitials in the first two layers were zero. This was because all purely repulsive atoms in these first layers escaped the lattice completely. The other positive levels shown, were incomplete, because many interstitial positions did not possess stable energy levels. The unstable levels oscillated because of significant lattice motion, caused by crowdion migration, and measured by a short range potential. The range was so short, that significant jumps in binding energy occured when an atom moved into, or out of the range of the potential. Evidently,

small vibrations in atoms with an equilibrium distance of about $\sqrt{3}$ LU from the interstitial, frequently caused crossings of this range limit, adding or subtracting energy from the binding energy each time one of them crossed, thus invalidating many of the interstitial binding energies.

The energy levels shown, however, demonstrated the meaning of a positive "binding energy". The numbers reflected the "amount of repulsion" associated with different positions in the lattice. The ordering of the levels, i.e., higher energies for deeper layers was expected. An interstitial deeper in the lattice felt more repulsion, because it was surrounded by a greater number of repulsive neighbors. Again, the level labeled "∞" represented an interstitial in a 14 x 14 x 14 lattice; but in this case of a Method 2 interstitial, crowdion migration did not occur.

The concept of a positive binding energy may or may not be the actual physical situation, but it is still academically valuable. Instead of an atom resting near the bottom of a potential well, as in Method 1, an atom can be "wedged" between the repulsive walls of its neighbors. In both cases, the atom is "bound" in the lattice. The ordering, spacing, and other correspondences between the positive and negative levels validate the qualitative use of the positive levels.

2. <u>Replacement Impurities</u>

A tungsten lattice with a replacement impurity is a perfect tungsten lattice, but Method 1 or Method 2 could be used on the atom in question. For Method 1, a perfect crystal was allowed to relax with time, yielding only negligible motion; and the

binding energies of the center atom in each layer was recorded (see Figure 1). The binding energies of atoms in the first, second, and third layers were -5.3 eV, -6.8 eV, and -7.0 eV respectively. The subsequent reversal of order for levels corresponding to deeper layers is a program anomally, caused by the use of a finite depth crystal. Runs on larger crystals indicated that the order would not reverse in an infinite lattice. The "∞" level at -8.8 eV is the experimentally determined heat of sublimation [26] of tungsten. These numerical values for the binding energies were valid as standards of comparison for the Ne-W data, since the motion and equilibrium positions of the replacement atoms and their neighbors were nearly identical, and usually less than .3 LU in both cases. Note that the binding energies of the Method 1 replacement atoms were lower than the interstitial atom levels. As previously stated, this was to be expected, since a replacement atom rests in the bottom of a periodic potential well in the lattice, whereas an interstitial rests in a higher well, because it is nearer to its neighbors than the normal equilibrium separation. Also note that if the entire Method 1 spectrum of binding energy levels were used as a standard of comparison for Ne-W levels, then the W-W interstitial levels should be higher with respect to the replacement levels, than shown in Figure 1, because of crowdion migration.

The Method 2 replacement level labeled "∞" corresponded to a replacement atom in the center of the fifth layer in a 10 x 10 x 10 lattice. Note that it was not above the interstitial levels, as it should have been by comparison with Method 1. This

was the major weakness of Method 2: because it was a measure of repulsion only, and neglected the potential well, it under estimated the values of the binding energies of atoms whose normal position was in that well; i.e., replacement defects.

E. THE NEON DEFECT IN TUNGSTEN

The neon atom defect was again placed in any one of the three lattice positions, labeled "int A", "int B", and "rep". The neon defect could be treated by Method 2 only. The neon energy levels are shown in Figure 2, on the next page. Note that the energies have been multiplied by a mass correction factor. (See Appendix D.)

1. Interstitials

The neon interstitial never initiated crowdion migration, but as in the W-W case, atoms placed in the first two layers escaped the crystal, and therefore had zero binding energy. Again, the ordering of the levels was a measure of the replusion on the interstitial, which increased as the interstitial was placed deeper in the lattice. Again the "∞" level was the result of placing a neon interstitial in the center of a 14 x 14 x 14 tungsten lattice.

2. Replacement Impurities

Again note that the replacement levels are lower than would be expected by comparison to the W-W Method 1 standard. It is hypothisized that these replacement levels should be higher than the interstitial levels, by comparison to the standard. This assumption is valid if a Ne-W potential well exists. It is feasible that since neon is almost incapable of binding, that no Ne-W well exists. On the other hand, the ionization state of both neon

FIGURE 2.

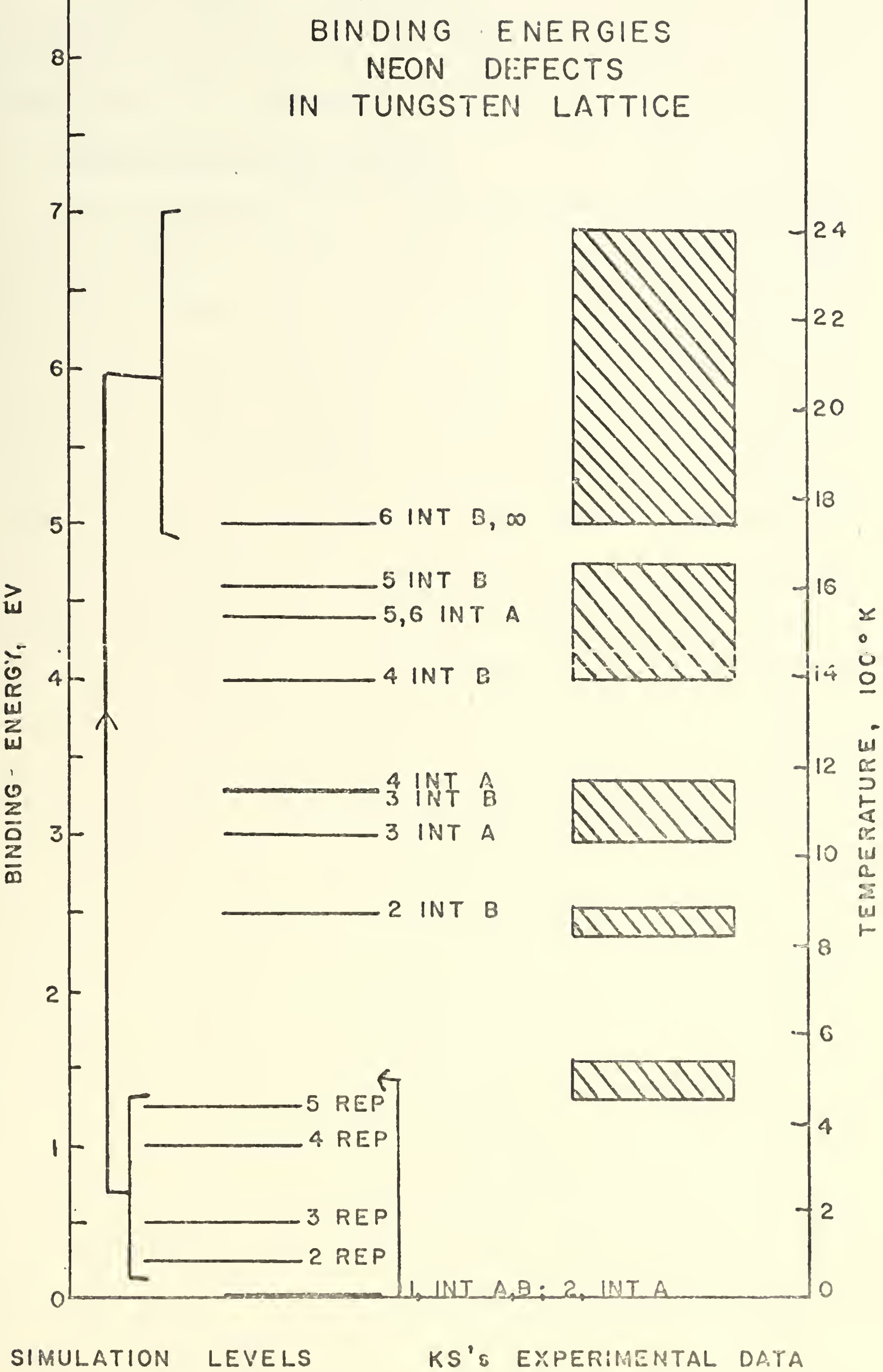
BINDING ENERGIES
NEON DEFECTS
IN TUNGSTEN LATTICE
BINDING - ENERGY, EV
0
1
2
3
4
5
6
7
8
6 INT B, ∞
5 INT B
5,6 INT A
4 INT B
4 INT A
3 INT B
3 INT A
2 INT B
5 REP
4 REP
3 REP
2 REP
1, INT A,B; 2, INT A
TEMPERATURE, 10C° K
0
2
4
6
8
10
12
14
16
18
20
22
24
SIMULATION LEVELS
KS's EXPERIMENTAL DATA

and tungsten in the lattice is unknown, so the existence of a shallow potential well is quite possible.

F. CORRELATION WITH EXPERIMENT

1. Scaling the Levels and Peaks

Since no <u>direct</u> way of transforming the Ne-W energy levels into correctly scaled negative values exists, an arbitrary linear scaling factor between KS's data and the Ne-W levels has been used. Note that every level or group of levels corresponded to an experimental peak in Figure 2, except in two places: first, the broad peak at about 2000° K had no energy level counterpart, but could be assumed to correspond to the closely ordered replacement levels, shifted above the interstitial levels by the above hypothesis. Second, the narrow peak at 450°K was without an energy level counterpart. Note that three interstitial levels had zero simulated binding energy because they had escaped the crystal. If, however, the assumption that a Ne-W well exists was true, then some or all of these three interstitial locations, (i.e., two surface layer positions and the open channel position in the second layer) would be stable, bound positions, and would be expected to generate an energy level in the vacinity of the 450° K peak. If the arbitrary scaling of the peaks and levels was correct, then the peak at 450° K is proof that a Ne-W well exists, since a purely repulsive potential would not allow a first layer or second layer open channel interstitial energy level to exist. The existence of this well, then, would in turn substantiate the shift of the replacement levels above the interstitial levels, to correspond to the 2000° K peak.

2. Probes of Potential Wells

Various attempts to substantiate the scaling between the levels and peaks were made. No approximation to a Ne-W potential well could be justified, and the correspondence between W-W and Ne-W results was not complete enough to invert and scale the potential energy levels to realistic, negative, binding energies.

Attempts were also made to match both Method 1 and Method 2 W-W energy levels to KS's data. The Method 2 levels were too incomplete, and the Method 1 levels required an unknown arbitrary reduction of interstitial energy levels to compensate for crowdion migration. Too many alternate reductions were possible to choose one as the correct rescaling.

Another approach that yielded little information was a plot of the differences between interstitial and replacement energy levels for each layer in the lattice.

One valuable method of investigating the nature of possible Ne-W negative binding energies was to probe the perfect lattice with an interstitial at various initial positions and plot the resultant potential energy of an interstitial vs. position. Since the potential was always positive, the results of this investigation were potential wells above the x-axis. Although the positive location of these wells was not realistic, the relative depth of the wells was significant. The average depth of a neon interstitial well, deep in the lattice, was about 4.2 eV (see Figure 8). The graph was made by placing interstitials in positions in the ⟨010⟩ open channel, and thus represents the barriers that the interstitial must penetrate as it escapes the crystal. Note that the wells were not at the obvious holes in the BCC lattice, but were between layers.

In the actual simulation, the interstitial rarely fell into this well, but instead pushed its two nearest neighbors away and made the <u>initial</u> position the low potential position. Here again, surface effects and relaxation reduced the tendency for interstitials to relax into expected infinite lattice equilibrium positions. Slight differences in the final equilibrium positions were not of significant importance to binding energies. The actual numerical values for the depths of these positive wells were not necessarily scaled properly since they ignored the actual Ne-W potential well, and were found from perfect lattice probes at time zero, before relaxation. Nevertheless, the depth of a well deep in the lattice of 4.2 eV agreed well with KS's prediction of 4.5 eV [8] for the desorbtion energy corresponding to $1720^{\circ}K$, at the front edge of the highest peak. $1720^{\circ}K$ closely approximated the temperature that the arbitrary scaling had assigned to a deep interstitial.

Note that the initial position of a replacement atom was $\sqrt{3}$ LU from its neighbors, and thus because of potential erosion, it had a potential of zero eV initially. To climb out of this well, about 17.5 eV must be supplied. Although this number was inaccurate for the same reasons listed above, it did demonstrate that even a purely repulsive potential <u>can</u> predict a greater binding energy for replacement atoms than for interstitial atoms.

V. CONCLUSIONS

An arbitrary scaling has been used to correlate the simulation results with experimental data. Although the method was not analytically sound, no other avenues of approach to the problem could be found that could further justify our hypothesis.

Satisfaction can be gained, however, from the fact that these results compare favorably with known data at many interfaces. Our model was a tried and proven one, with many successful sputtering, channelling, and similar simulations to its credit. This present model invariably behaved in a physically valid manner or a manner which could be made physically acceptable by varying the controlling parameters in the program. Specifically, many previous experimental and simulated results for infinite crystals were reproduced when simulation took place deep in a large lattice, such as the ⟨110⟩ split interstitial position for BCC structures. The Method 1 replacement levels, if found for a much deeper crystal, would have asymptotically approached very close to the 8.8 eV heat of sublimation. The simulated depth of the positive potential well for interstitials of about 4.2 eV closely approximated KS's prediction of 4.5 eV.

All avenues in additional computer simulation have not been exhausted. Future simulation of Argon, Krypton, and Xenon defects in tungsten should be fruitful. Comparisons between the relative locations of these new energy levels might further substantiate this research. In particular, if simulation can explain why KS's neon data contains five desorbtion peaks, while their Argon, Krypton, and Xenon data contain four peaks, it will be a major

success. KS also gathered data for different crystal surfaces and different angles of incidence, which might be investigated by computer simulation.

This simulation was also important in that it investigated the lattice surface; a topic which has not received as much attention as infinite crystal dynamics. Since radiation damage theory and modern transistor theory is very much concerned with the crystal surface, the computer simulation field will undoubtably increase their emphasis on surface effects, with considerable attention toward better ways of treating a foreign interstitial.

A new exhaustive book which reports on the present state of knowledge in all these areas, with emphasis on experimental results has just been published. It is a report on the proceedings of the International Conference on Vacancies and Interstitials in Metals, 1968 [27].

APPENDIX A: CRYSTAL GEOMETRY

The computer program can call any one of nine lattice generator subroutines: three face-centered cubic subroutines ([L100], [L110], [L111]), three body-centered cubic subroutines ([B100], [B110], [B111]), and three diamond subroutines ([D100], [D110], [D111]). The diamond subroutines are never used and therefore not compiled; but provision has been made for their future inclusion in the program. The dimensions of the lattice chosen were controlled by the input data variables [IX], [IY], and [IZ]. Each atom in the crystal was numbered, in the order x followed by z, followed by y. For the surface layer (Y = 0) of the tungsten 10 x 10 x 10 lattice, atoms were numbered from 2-26; for the first layer below the surface, atoms were numbered 27-51, etc. Atom number 1 was the primary, or point defect atom. [LD] was the number of the last mobile atom, or the last atom in the eighth layer, number 200; and [LL] was the number of the last atom in the crystal, number 250.

The placement of point defects was accomplished as follows: after the desired perfect lattice was built to the desired size, subroutine PLACE was called. Three types of defects were allowed: vacancies, interstitials, and replacement impurities. The type and location of the defect were controlled by input data variables: the type of defect [ITYPE], an atom number [NVAC] and a displacement vector [D1X, D1Y, D1Z] in LU. If [ITYPE] = 1, a vacancy was created in site number [NVAC]. This "removal" was accomplished by setting [LCUT (NVAC)] = 1 which "turned off" the atom, removing it from all calculations. If [ITYPE] = 2, an interstitial was created in a position [-DIX, -DIY, + DIZ] LU from

site number [NVAC]. This interstitial was always atom number 1. Since atom number 2 was always at the origin, number 1 could be placed using a displacement vector from the origin (from [NVAC] = 2) or using a displacement vector from a site next to the interstitial. If [ITYPE] = 3, a vacancy was created in site number [NVAC] and a replacement impurity, put in its place. Note that for both [ITYPE] = 2 and 3, either a foreign or self defect could be placed. For the case of either the self-interstitial or the self-replacement atom (giving us back the perfect crystal), either method 1 or method 2 of calculating the potential could be used. The choice of methods was also an input parameter: for method 1, [IQ] = 1, and for method 2, [IQ] = 2.

APPENDIX B: POTENTIALS

(In this appendix and all subsequent appendices, the brackets denoting program language are dropped. Program language is still written in all capital letters.)

A. BORN-MAYER REPULSIVE POTENTIAL

1. Potential Energy: For the lattice atom interactions, the Born Mayer potential equation is:

$$V_{ij} = \exp(A + Br_{ij}) \quad (1)$$

or

POT = EXP(EXA + EXB*DIST) (1A)

For bullet-lattice atom interactions,

$$V_{ij} = \exp(A' + B'r_{ij}) - V_{ij}(ROE) \quad (3)$$

where $V_{ij}(ROE)$ is subtracted to retard the potential so that it goes to zero at the nearest neighbor distance. In the program, the V_{ij} equation is:

POT = EXP(PEXA + PEXB*DIST) - PPTC (3A)

2. Force: For the lattice atom interaction,

$$\text{Force} = \frac{-\partial V_{ij}}{\partial r_{ij}} = -B \exp(A + Br_{ij})$$

$$= \exp\left[(\ell n\ -B + A) + Br_{ij}\right] \quad (4)$$

in the program, $\ell n(-B + A)$ = (ALOG[-EXB*CVED]+ EXA) = FXA, where CVED is a conversion factor for units, and

FORCE = [FXA + EXB*DIST] (4A)

For bullet-lattice atom forces,

$$\text{Force} = \frac{-\partial V_{ij}}{\partial r_{ij}} = -B'\exp(A'+B'r_{ij}) = \exp[\ell n\text{-}B'+A')+B'r_{ij}] \quad (5)$$

where $(\ell n\text{-}B'+A')$=(ALOG[-PEXB*CVED]+PEXA) = PFXA, and

FORCE = EXP[PFXA + PEXB*DIST] (5A)

For bullet-lattice atom forces for which lattice atoms enter the range of the bullet's force during the timestep, a first approximation to the force is given by:

$$\text{Force} = \frac{V_{ij}-V_{ij}(\text{ROE})}{r_{ij}-\text{ROE}} \quad (6)$$

(See Figure 9). $V_{ij}-V_{ij}(\text{ROE})$ is the retarded potential given above. A conversion factor is needed to preserve the proper units, so the following substitutions are made in the retarded potential equation (3A): (PEXA) becomes (ℓn CVED+PEXA) = PAC, so V_{ij} = EXP[PAC+PEXB*DIST], and $V_{ij}(\text{ROE})$ = PPTC becomes PFPTC, which is $V_{ij}(\text{ROE})$ calculated after the PAC substitution. Finally, r_{ij}-ROE = DIST-ROE = DFF, and

$$\text{FORCE} = \frac{(\text{EXP[PAC+PEXB*DIST]} - \text{PFPTC}}{\text{DFF}} \quad (6A)$$

Note: (5A) is used for 0 ≤ DIST ≤ ROE - DT1 = ROEM, and (6A) is used for ROEM < DIST < ROE.

B. MORSE POTENTIAL

1. <u>Potential Energy</u>: For lattice atom interactions, the Morse potential equations is:

$$\Phi_{ij} = D[\exp\{-2\alpha(r_{ij}-r_o)\}-2\exp\{-\alpha(r_{ij}-r_o)\}] \quad (2)$$

$$= \exp[(\ell n D + 2\alpha r_o)-(2\alpha)r_{ij}]-\exp[(\ell n(2D)+\alpha r_o)-(\alpha)r_{ij}]$$

= EXP[(ALOG(DCON)+ 2.*ALPHA*RE) -(2.*ALPHA*CVR)*DIST]

- EXP[(ALOG(2.*DCON)+ ALPHA*RE) -(ALPHA*CVR)*DIST]

= EXP[CGD1-CGB1*DIST]- EXP[CGD2-CGB2*DIST] (2A)

2. <u>Force</u>: For lattice atom interactions,

$$\text{Force} = \frac{-\partial\phi_{ij}}{\partial r_{ij}} = D[2\alpha\exp\{-2\alpha(r_{ij}-r_o)\}-2\alpha\exp\{-\alpha(r_{ij}-r_o)$$

$$= \exp[\ell n(2\alpha)+(\ell n D+2\alpha r_o)-(2\alpha)r_{ij}]-\exp[\ell n\alpha+(\ell n(2D)+\alpha r_o)-(\alpha)r_{ij}]$$

= EXP[ALOG(2*ALPHA*CVR*CVED)+ALOG(DCON)+2.*ALPHA*RE

-(2.*ALPHA*CVR)*DIST]

- EXP[ALOG(ALPHA*CVR*CVED)+ALOG(2.*BCON)+ALPHA*RE

-(ALPHA*CVR)*DIST]

= EXP[ALOG(-CGB1*CVED)+CGD1)-CGB1*DIST]

- EXP[(ALOG(-CGB2*CVED)+CGD2)-CGB2*DIST]

= EXP[CGF1-CGB1*DIST]- EXP[CGF2-CGB2*DIST] (7A)

C. CUBIC FIT

1. Potential Energy: The best cubic fit between the BM and Morse potentials is calculated in Subroutine CROSYM. The potential equation, defined between ROEA and ROEB, is

$$POT = CP3r_{ij}^3 + CP2r_{ij}^2 + CP1r_{ij} + CP\emptyset \quad (8)$$

or POT + DIST*(DIST*(DIST*CP3+CP2)+CP1)+CPØ (8A)

2. Force: $Force = \frac{-\partial POT}{\partial r_{ij}} = -3CP3r_{ij}^2 - 2CP2r_{ij} - CP1 \quad (9)$

$$= (-3.*CP3*CVED)r_{ij}^2+(-2.*CP2*CVED)r_{ij}+(-CP1*CVED)$$

$= CF2r_{ij}^2 + CF1r_{ij} + CF\emptyset$, or

FORCE = DIST*(DIST*CF2+CF1)+CFØ. (9A)

APPENDIX C: AVERAGE FORCE METHOD AND TIME DURATION THEORY

A. AVERAGE FORCE METHOD: The average force technique has been explained in great detail in Ref. 15. It was summarized in Chapter 3, and therefore discussion here is limited to the average force method in the program language.

When the desired lattice is built, the position of the ith atom is stored simultaneously in RX(I), RY(I), RZ(I); RXK(I), RYK(I), RZK(I); and RXI(I), RYI(I), RZI(I). The latter set of coordinates never change and are used for comparing new positions to original positions, and in calculating DX(I), DY(I) and DZ(I) for output. The middle set of coordinates containing the letter K are for storing the initial positions at the beginning of each timestep.

A step by step summary of the average force method, showing X coordinate calculations only, follows:

1. Based on the position, RX(I), of the ith particle at the beginning of the timestep, the force FX(I) is calculated in STEP.

2. RX(I) is stored in RXK(I).

3. The new, temporary position, RX(I) is calculated, based on the force at RXK(I):

$$X^1 = X + V\Delta t + F(\Delta t)^2/2m \qquad (10)$$

or

$$RX(I) = RX(I)+DTOD*(HDTOM*FX(I)+VX(I). \qquad (10A)$$

4. A new force is calculated, based on this new position RX(I).

5. VSS stores VX(I), the original velocity of the ith atom. This velocity is half the velocity of the ith atom in the previous timestep: the ½ factor being an arbitrary damping multiplier. A

new velocity, based on the <u>new</u> force, is found:

$$V^1 = V + F\Delta t/2m \qquad (11)$$

or

$$VX(I) = VSS+HDTOM*FX(I). \qquad (11A)$$

6. The <u>final</u> position is calculated, based on the <u>average</u> of these two velocities

$$X^1 = X + \tfrac{1}{2}\Delta t(V+V^1) \qquad (12)$$

or

$$RX(I) = RXK(I)+(VX(I)+VSS)*HDTOD \qquad (12A)$$

The resultant velocities are halved, a new timestep duration is calculated, and the process repeated.

B. TIMESTEP DURATION THEORY

This simulation uses the best possible estimate of a timestep duration, DT, as calculated from the <u>present state</u> of the forces and energies in the lattice for use in the <u>next</u> timestep. To limit motion to an increment small enough to preserve the accuracy of the average force approximation, we define DTI as the maximum distance any atom is allowed to move in one timestep.

From (10), we find

$$\Delta X_i = (V_i + F_i\Delta t/2m)\Delta t.$$

Therefore,

$$\Delta t = \Delta X_i/(V_i+F_i\Delta t/2m). \qquad (13)$$

For

$$V_i >> F_i\Delta t/2m, \quad \Delta t \doteq \Delta X_i/V_i. \qquad (14)$$

If we find the fastest moving atom and assure that it does not move more than DTI, we have limited the motion of all other atoms to less than DTI.

Thus,

$$DT = (DTI*CVD)/EMAX = FDTI/EMAX \qquad (14A)$$

where

$$EMAX = SQRT(VX(I)*VS(I)+VY(I)*VY(I)+VZ(I)*VZ(I).$$

For $\qquad V_i >> F_i \Delta t/2m,$

$$\Delta t = \Delta X_i/F_i \Delta t/2m = \frac{2m\Delta X_i}{F_i} \quad . \qquad (15)$$

Anatagous to above, we find the most stressed atom and assure that it does not move more than DTI. Thus,

$$DT = SQRT[(2.*PTMAS*DTI*CVD)/FMAX]$$

$$= SQRT[TFAC/FMAX] \qquad (15A)$$

where FMAX= SQRT[FX(I)*FX(I)+FY(I)*FY(I)+FZ(I)*FZ(I)].

Since rigorously we cannot make either or these limiting assumptions, we must go back to our original equation for DT, equation (13). Since this equation involves DT, we proceed as follows:

1. Assume $V_i << F_i \Delta t/2m$ and calculate Δt from (15A).

2. Insert this preliminary value for DT in (13) and compare V_i to $F_i \Delta t/2m$. If V_i is larger, calculate DT from (14A). If $F_i \Delta t/2m$ is larger calculate DT from (15A).

A complication arises when a foreign impurity is in the lattice, because of a variation in the value for m in (15). This is especially acute when the differences in masses are great. The method used to solve this problem is as follows:

1. If <u>either</u> FMAX = F_1 <u>or</u> EMAX = V_1, the entire proceedure, above, is followed using the mass of the bullet for m.

2. If both FMAX $\neq F_1$ and EMAX $\neq V_1$, the entire proceedure is followed using the mass of a lattice atom.

The requirement that the bullet mass be used if either EMAX or FMAX describe the bullet circumvents the problem of having the

bullet the fastest moving atom, but <u>not</u> the most stressed atom, or visa versa.

To begin the problem, an arbitrary value of 10^{-14} seconds is assigned to DT. If at any time in the program EMAX = FMAX = zero, 10^{-14} is again assigned to DT to prevent division by zero.

APPENDIX D: SUBROUTINES STEP, ENERGY, AND LOCAL

A. DISTANCE CALCULATIONS

In all three subroutines, STEP, ENERGY, and LOCAL, a method of finding all atoms within a given radius of another atom was needed. For lattice atom interactions, atoms inside ROEA, ROEB, and ROEC were found; for the foreign interstitial interactions, atoms inside ROE were found; and for LOCAL, atoms inside ROEL of a point defect were found. The time saving technique used to do this was to successively eliminate all atoms with an x component difference greater than the given radius, then similarly for y components, then for z components. The resulting volume not eliminated is a cube circumscribing the desired sphere. Finally the time-consuming test of eliminating all atoms for which the desired radius is less than SQRT (DRX*DRX + DRY*DRY + DRZ*DRZ) is applied to only atoms inside the cube.

B. SUMMATION INDICES IP AND IQ

Interactions V_{ij}, $\emptyset_{ij}$, and F_{ij} are found by evaluating all values in the half matrix. For example F_{12}, F_{13}, F_{14} $\cdots$ are found, then F_{23}, F_{34}, $\cdots$ etc. The variable IP controls the starting point for the j summation. IP is always set to I + 1 to avoid the repetition of finding F_{ij} and F_{ji}. IQ controls the starting point for the i summation. If the primary is to be treated as a lattice atom, IQ = 1. If it is to be treated as a foreign particle, IQ = 2, and all F_{ij} are found separately.

C. DISTRIBUTION OF FORCES AND POTENTIAL ENERGIES

The forces F_{ij} are equal and opposite on i and j: i.e., $F_i = -F_j$. The potential energies are split in proportion to the reduced

mass of the interacting particles. This is easily understood by observing the kinetic energy distribution of an elastic collision of m and M where M > m. We find that m carries away almost all the kinetic energy: specifically it carries away $\left(\frac{M}{m+M}\right) E_{TOT} \sim E_{TOT}$. If a pair of atoms are to behave elastically, the potential energies which are transformed into kinetic energies of motion must be split in the same manner. For this reason,

$$PPE(1)=\left(\frac{TMAS}{TMAS+BMAS}\right) * POT = BSAVE*POT;$$

and

$$PPE(J)=\left(\frac{BMAS}{TMAS+BMAS}\right) *POT = TSAVE*POT.$$

note, for BMAS = TMAS, BSAVE = TSAVE = ½, and the energies are split equally.

D. SUBROUTINE LOCAL

LOCAL measures the change in potential energy associated with a sphere of radius ROEL surrounding a point defect. It sums up the potential energies of each atom found inside this sphere at time zero. It remembers these atoms, and for each timestep re-sums the potential energies of these same atoms. The sum, total local potential energy TLPE, is subtracted from TLPE at time zero (TLPEØ), to give a measure of the change in potential energy (DLPE) inside ROEL.

APPENDIX E: COMPUTER PROGRAM GLOSSARY

NOTE: In this glossary, the terms "point defect atom", "bullet", and "primary" are synonymous; and the terms "lattice atom" and "target" are synonymous.

ALPHA: Input Morse potential parameter

BSAVE: Target mass/(target mass + bullet mass); distributes potential energy between target and bullet

BIND: Negative of the total potential energy (TPOT) at time zero

BMAS: Mass of bullet in amu

BULLET: Alpha-numeric array for point defect material

CFO, CF1, CF2: Force parameters of cubic fit between Morse and Born-Mayer functions

CGB1, CGB2: Morse potential parameters

CGD1, CGD2: Morse potential parameters

CGF1, CGF2: Morse force parameters

CPO, CP1, CP2, CP3: Potential parameters of cubic fit between Morse and Born-Mayer functions

CVD: CVR x 10^{-10}, converts lattice units to meters

CVE: 1.6 x 10^{-19}, converts electron volts to joules

CVED: CVE/CVD, a ratio used to avoid repeated division

CVM: 1.672 x 10^{-27}, converts atomic mass units to kilograms

CVR: LU in angstroms; converts lattice units to angstrom units

D1X, D1Y, D1Z: Displacement coordinates for location of interstitial from reference atom, NVAC

DCON: Input Morse potential parameter

DFF: ROE-DIST, the distance closer than ROE that an atom is to the primary

DIST: Distance between any two atoms

DLPE: TLPE-TLPEØ, the change in total local potential energy since time zero

DRX, DRY, DRZ: x,y,z components of DIST

DT: Length of a timestep in seconds

DTI: Number of lattice units most energetic atom may move in one timestep

DTOD: DT/CVD--a ratio used to avoid repeated division

DTOM: DT/PTMAS--a ratio used to avoid repeated division

DTOMB: DT/PEMAS--a ratio used to avoid repeated division

DX(I), DY(I), DZ(I): Change in position of ith atom from initial position at time zero

EMAX: The maximum energy encountered in any cycle

EV: Primary energy in electron volts

EVR: Primary energy in kilo-electron volts

EXA, EXB: Input Born-Mayer potential function parameters for the target

F2: Square of the force on a specific atom

FA: The component force increment on an atom

FDTI: DTI X CVD, a parameter used to determine DT my maximum energy method

FM: A small number used in checking potential energy zero point

FM2: FM squared

FMAX: Maximum total force on the most stressed atom in the crystal

FOD: FORCE/DIST--a ratio used to avoid repeated division

FORCE: Numerical value of the force function with a variable parameter

FX(I), FY(I), FZ(I): x,y,z components of total force on an atom

FXA: Born-Mayer force function parameter

HBMAS: ½ BMAS--a ratio used to avoid repeated division

HDTOD: ½ DTOD--a ratio used to avoid repeated division

HDTOM: ½ DTOM--a ratio used to avoid repeated division

HDTOMB: ½ DTOMB--a ratio used to avoid repeated division

HTMAS: ½ TMAS--a ratio used to avoid repeated division

I1: Variable in cubic fit subroutine

I3: " " " " "

IDEEP: Number of mobile layers

IH1: Alpha numeric array for program title

IH2: " " " " Morse function parameters

IHB: " " " " bullet element

IHS: " " " " type and orientation of crystal

IHT: " " " " target element

ILAY: Same as IDEEP

IN: Odd-even integer used to determine atom site establishment

IP: Subscript value of atom. Used in subroutines STEP and ENERGY

IQ: Parameter that determines whether or not a self defect is to be given a repulsive potential or a composite attractive-repulsive potential

ISHUT: A parameter used to shut down the program

IT: Unscaled fixed point x coordinate used in lattice generation

ITT: Odd-even integer used to determine atom site establishment

ITYPE: Parameter used to determine the type of point defect: vacancy, interstitial, or replacement

IX, IY, IZ: Number of x,y,z planes of crystal

J2: Variable in the cubic fit subroutine

JJ: Parameter in the BCC(111) lattice generation subroutine

JT: Unscaled y coordinate used in crystal generation

JTS: Variable used to establish atom sites

JTT: " " " " " "

KF: Final K in LOCAT (K) assigned to an atom

KT: Unscaled z coordinate used to establish atom site

LCUT(I): Used to identify an ith atom which is not included in calculations

LD: The highest numbered atom in the mobile layers

LL: The highest numbered atom in the entire crystal

LOCAT(K): Dimensioned variable that remembers the numbers of the atoms within a radius ROEL of the primary at time zero

LS: Variable associated with each of the nine lattice generator subroutines

MCRO: One number higher than the order of the fit between the Born-Mayer and Morse potentials, always 4 in this simulation

ND: Data output increment, in numbers of timesteps

NEW: Parameter used to determine whether or not atom numbers have been stored in LOCAT(K)

NPAGE: Page numbering variable

NRUN: Parameter used to determine whether or not to read additional data cards

NS: Initial print statement timestep number

NT: Timestep number

NTT: Timestep number limit before shutdown

NVAC: An atom number used to establish point defects or used as a reference point for interstitial placement

PAC: Parameter for bullet force function correction

PBMAS: Primary mass in kilograms

PEXA, PEXB: Input Born-Mayer potential function parameters for the bullet-target interaction

PFPTC: Primary force function evaluated at ROE

PFXA: Primary force function parameter

PKE(I): Kinetic energy of the ith atom

PLANE: Alpha-numeric array for lattice orientation

POT: Potential energy between two atoms

PPE(I): Potential energy of the ith atom

PPTC: Primary potential function evaluated at ROE

PTE(I): Total energy of the ith atom (potential + kinetic)

PTMAS: Target mass in kilograms

RE: Input Morse potential parameter

RO: Spacing constant in FCC(110) lattice generation subroutine

ROE: Nearest neighbor distance

ROE2: ROE squared

ROEA: Maximum cut off for Born-Mayer potential

ROEB: Minimum cut off for Morse potential

ROEC: Maximum cut off for Morse potential

ROEC2: ROEC squared

ROEL: Radius inside of which local potential energy is found

ROEL2: ROEL squared

ROEM: ROE-DTI, region in which modification of repulsive force must be made

RX(I), RY(I), RZ(I): x,y,z coordinates of an ith atom at any time

RXI(I), RYI(I), RZI(I): x,y,z coordinates of an ith atom's initial position

RXK(I), RYK(I), RZK(I): x,y,z coordinates of temporary position of an ith atom during force cycle

SAVE: ½ POT

SCX, SCY, SCZ: x,y,z coordinate scale factors

SSCZ: A z scale factor used for the FCC(111) lattice generator subroutine

START: An optional timing variable, not used in this simulation

SUM: Variable in cubic fit subroutine

TARGET: Alpha-numeric array for target material

TSAVE: Bullet mass/(target mass + bullet mass); distributes potential energy between target and bullet

TE: Total energy of all crystal atoms (kinetic + potential)

TEMP: Temperature of lattice in degrees Kelvin. Not used in this simulation

TFAC: A time factor ratio used to determine DT by maximum force method

TFACB: TFAC for the bullet

THERM: Thermal energy of atom. Not used in this simulation

TIME: Elapsed problem time in seconds

TLPE: Total local potential energy of atoms within a radius ROEL

TLPEØ: TLPE at time zero

TMAS: Target atom mass in amu

TPKE: Total kinetic energy of all crystal atoms

TPOT: Total potential energy of all crystal atoms

VSS: Storage variable for velocity components

VX(I), VY(I), VZ(I): x,y,z components of ith atoms velocity

X, Y, Z: Unscaled coordinates used in crystal generation

YLAX(I): Relaxation in -y direction of ith layer in L.U.

ZP: Floating point form of JTT

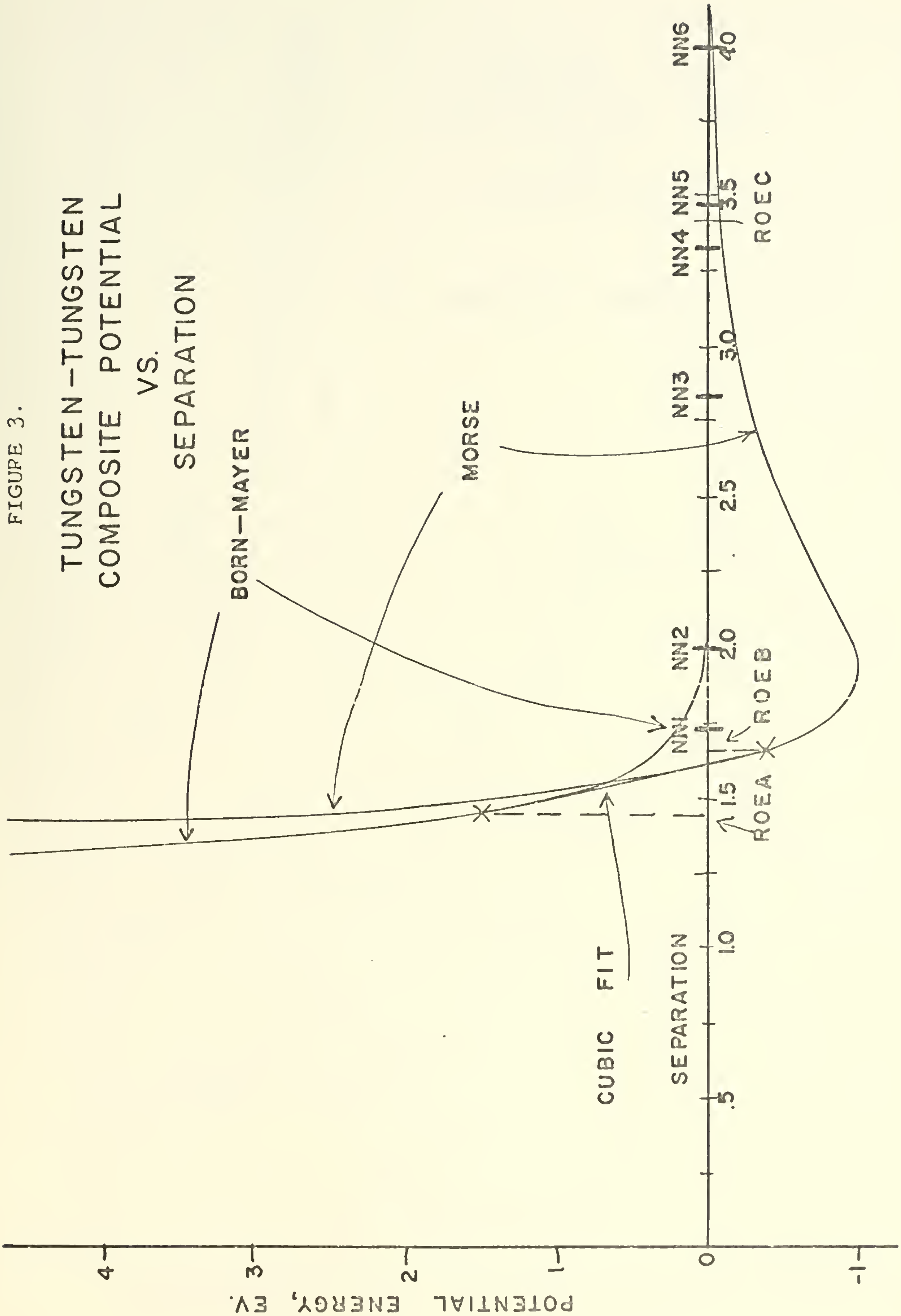

FIGURE 3.

TUNGSTEN-TUNGSTEN COMPOSITE POTENTIAL VS. SEPARATION

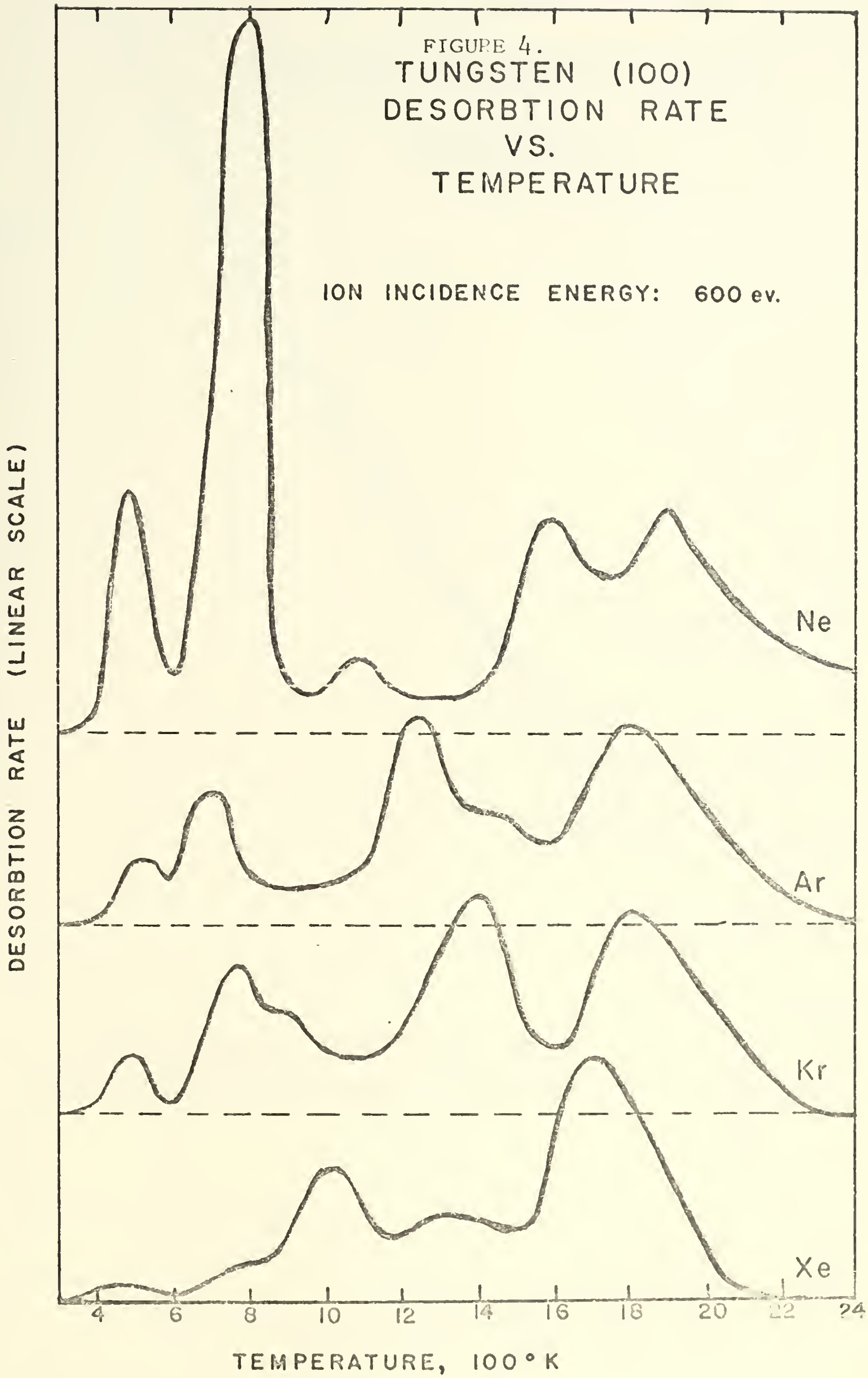
FIGURE 4.
TUNGSTEN (100)
DESORBTION RATE
VS.
TEMPERATURE
ION INCIDENCE ENERGY: 600 ev.
DESORBTION RATE (LINEAR SCALE)
Ne
Ar
Kr
Xe
4
6
8
10
12
14
16
18
20
22
24
TEMPERATURE, 100°K

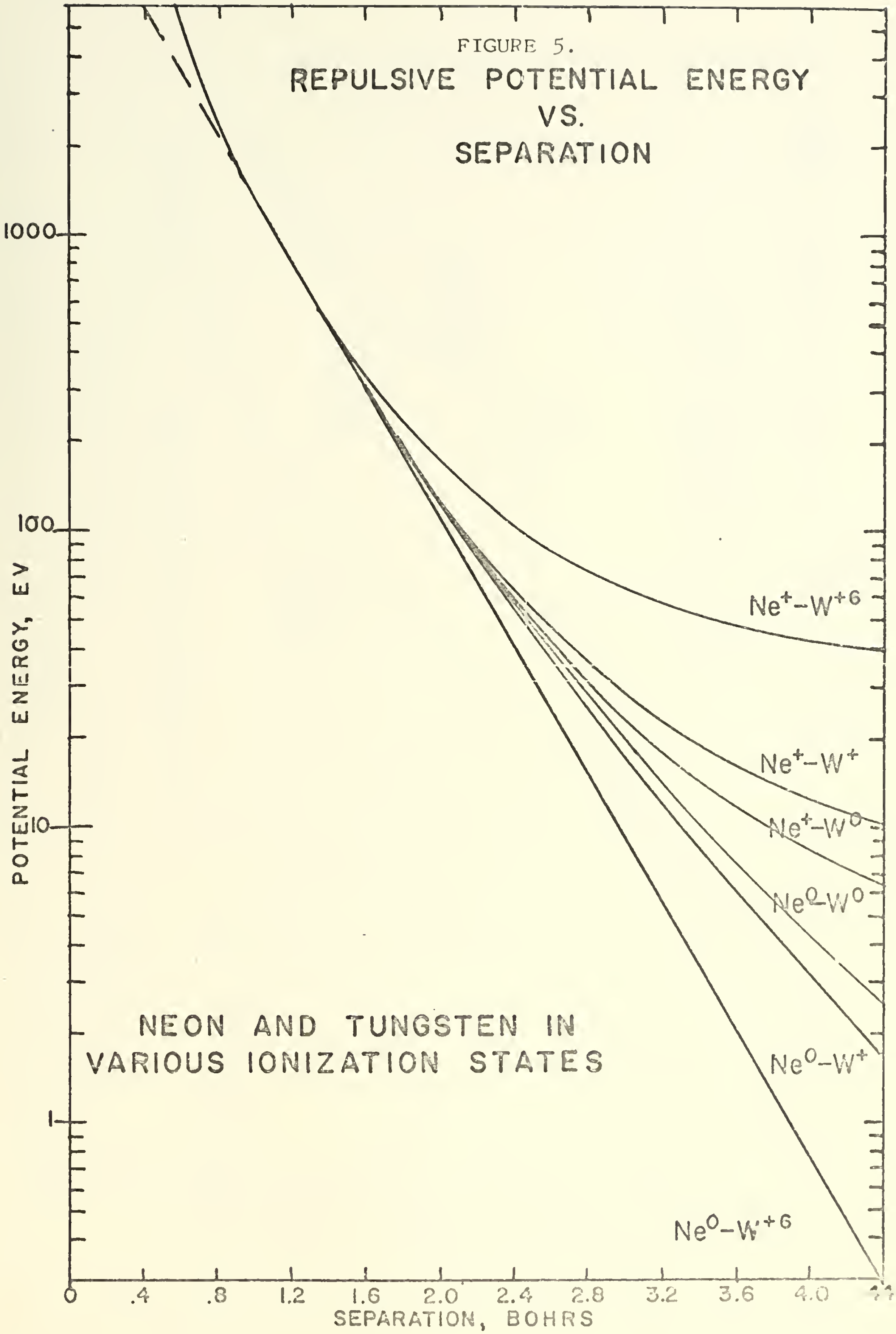
FIGURE 5.
REPULSIVE POTENTIAL ENERGY
VS.
SEPARATION
1000
100
10
1
POTENTIAL ENERGY, EV
$Ne^{+}-W^{+6}$
$Ne^{+}-W^{+}$
$Ne^{+}-W^{0}$
$Ne^{0}-W^{0}$
$Ne^{0}-W^{+}$
$Ne^{0}-W^{+6}$
NEON AND TUNGSTEN IN
VARIOUS IONIZATION STATES
0
.4
.8
1.2
1.6
2.0
2.4
2.8
3.2
3.6
4.0
SEPARATION, BOHRS

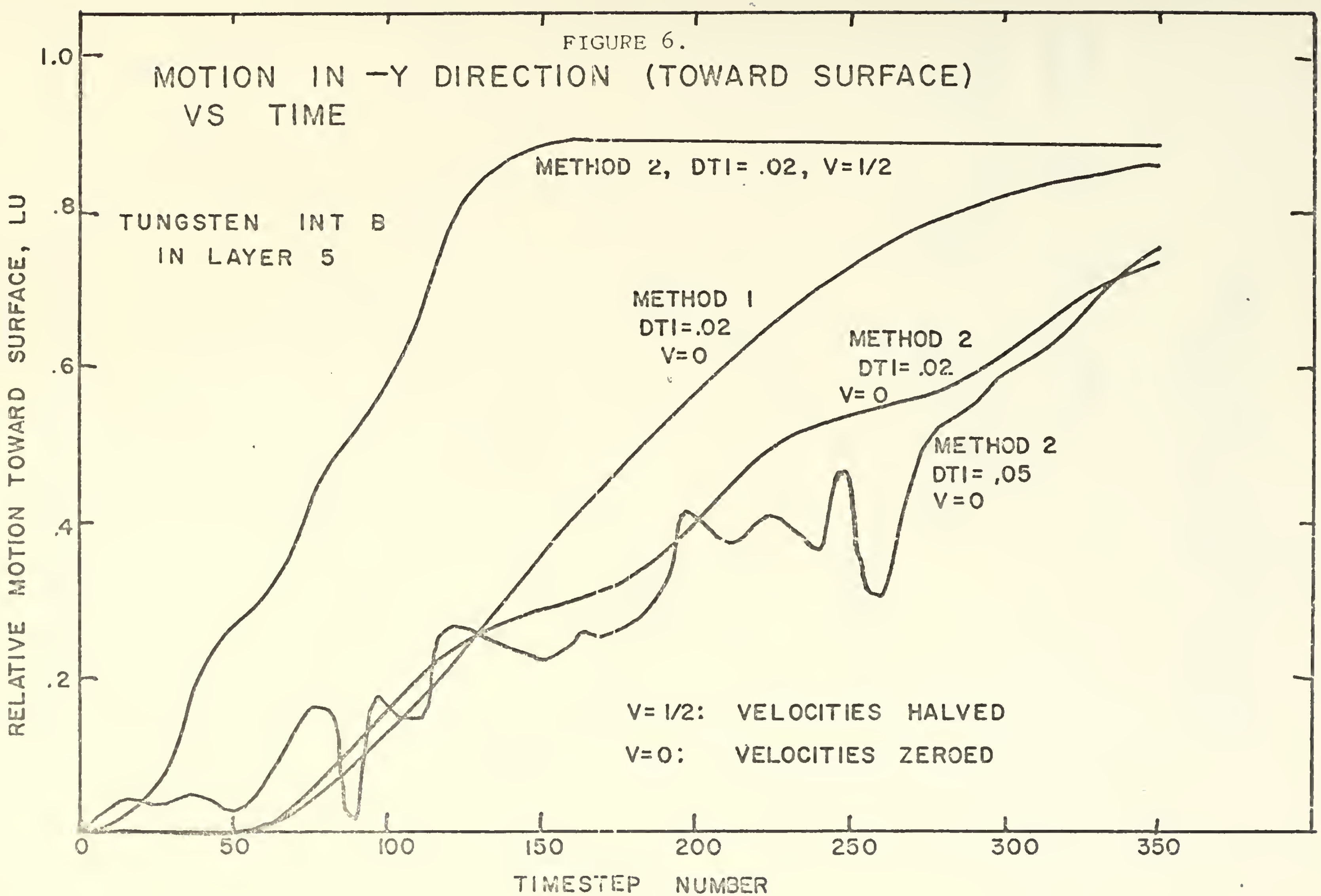
FIGURE 6.
MOTION IN −Y DIRECTION (TOWARD SURFACE)
VS TIME
TUNGSTEN INT B
IN LAYER 5
METHOD 2, DTI= .02, V=1/2
METHOD 1
DTI=.02
V=0
METHOD 2
DTI= .02
V= 0
METHOD 2
DTI= ,05
V=0
V= 1/2: VELOCITIES HALVED
V=0: VELOCITIES ZEROED
1.0
.8
.6
.4
.2
0
50
100
150
200
250
300
350
TIMESTEP NUMBER
RELATIVE MOTION TOWARD SURFACE, LU

FIGURE 7.

BCC (100) ORIENTATION
HARD SPHERE MODEL

SOLID LINE: "Y" PLANE
DASHED LINE: "Y−1" PLANE

INTERSTITIALS IN "Y" PLANE:
INT A IN <010> OPEN CHANNEL
INT B HIDDEN FROM SURFACE

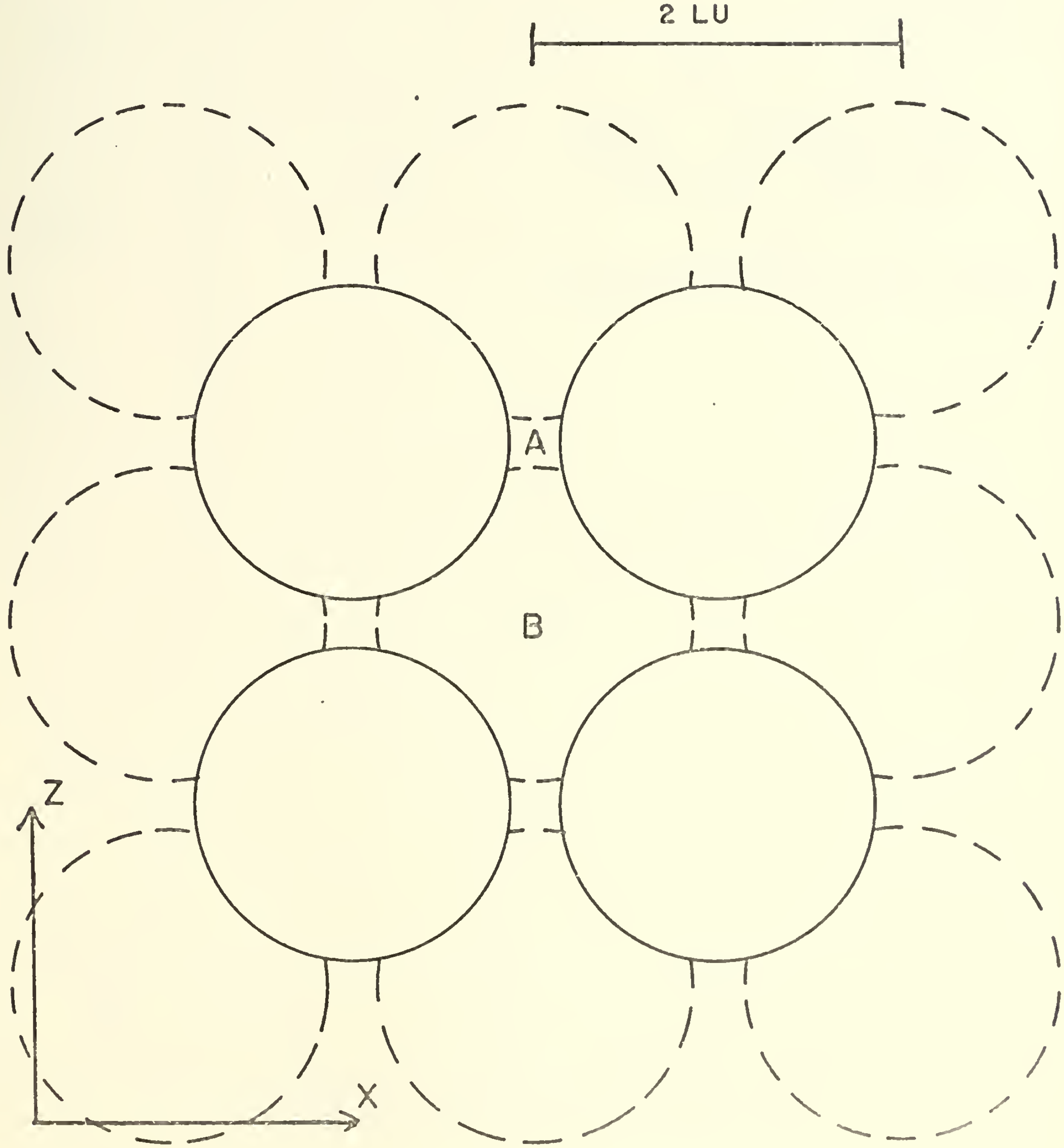

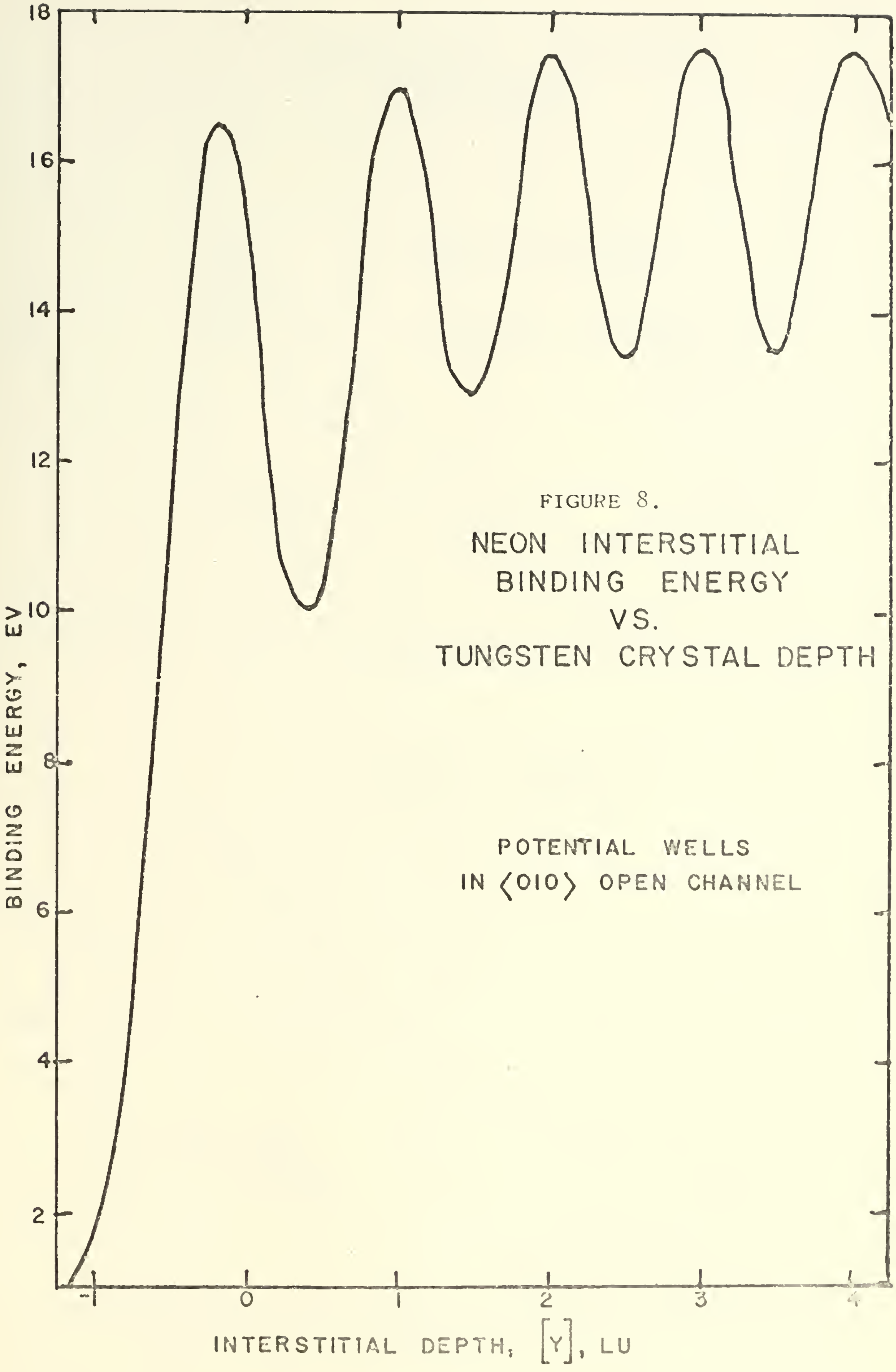
FIGURE 8.
NEON INTERSTITIAL
BINDING ENERGY
VS.
TUNGSTEN CRYSTAL DEPTH
POTENTIAL WELLS
IN ⟨010⟩ OPEN CHANNEL
BINDING ENERGY, EV
18
16
14
12
10
8
6
4
2
-1
0
1
2
3
4
INTERSTITIAL DEPTH, [Y], LU

FIGURE 9.

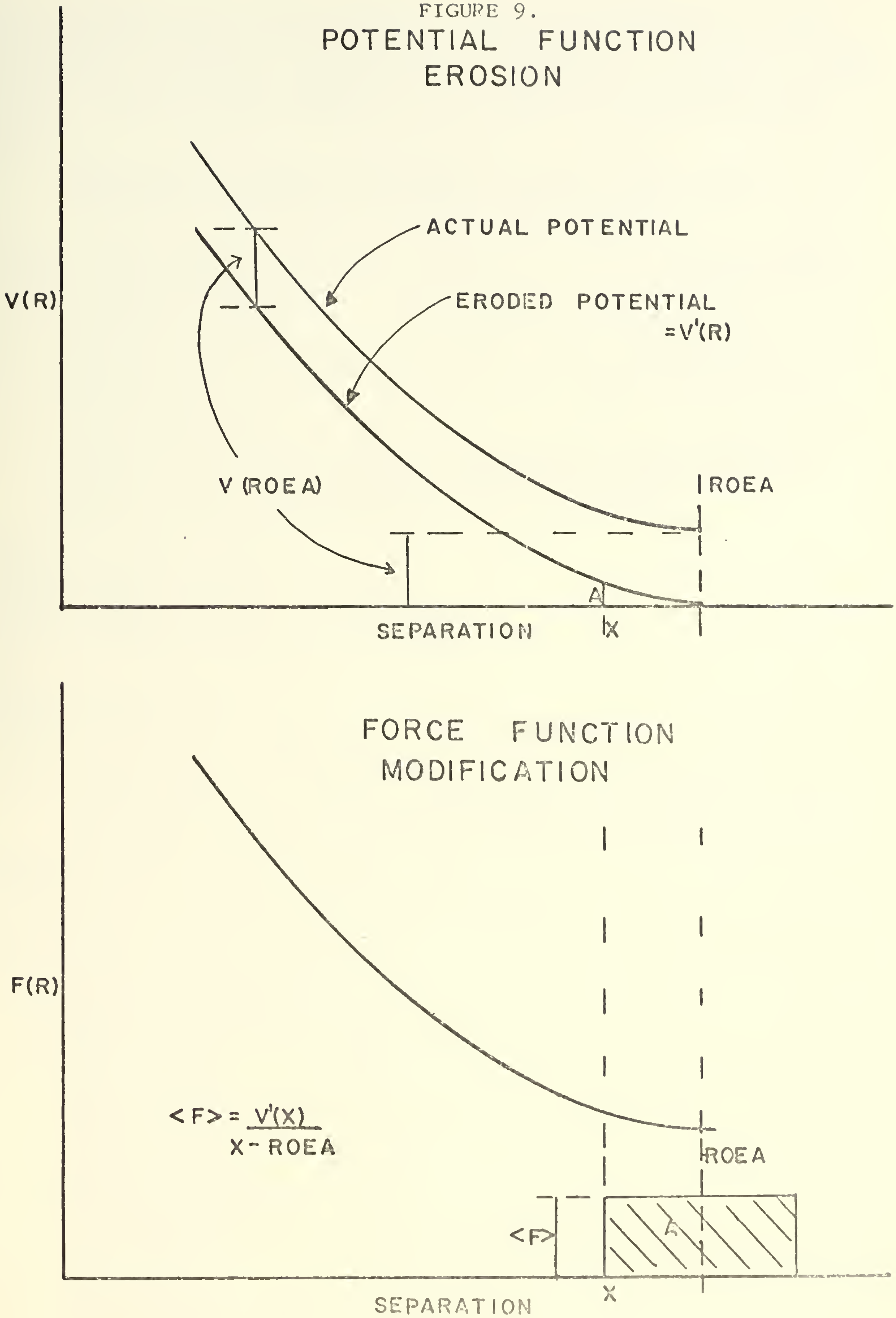

POTENTIAL FUNCTION
EROSION
ACTUAL POTENTIAL
ERODED POTENTIAL
=V'(R)
V(R)
V (ROEA)
ROEA
A
SEPARATION
X
FORCE FUNCTION
MODIFICATION
F(R)
<F> = V'(X) / X - ROEA
ROEA
<F>
A
X
SEPARATION

```
C
THIS PROGRAM GENERATES VARIOUS TYPES AND ORIENTATIONS OF
CRYSTAL LATTICES, AND INJECTS A VACANCY, INTERSTITIAL, OR
REPLACEMENT IMPURITY AT A DESIRED LOCATION.  IT THEN, BY USE
OF ATOMIC POTENTIAL PARAMETERS AND NEWTONIAN MECHANICS, CAL-
CULATES THE DYNAMIC RESULTS OF THE SYSTEM; OUTPUTING POS-
ITION, VELOCITY, AND ENERGY VALUES FOR EACH ATOM IN THE
CRYSTAL.
C
DIMENSIONING OF VARIABLES NOT NEEDED IN COMMON
      DIMENSION VX(1000),VY(1000),VZ(1000),PKE(1000)
      DIMENSION DX(1000),DY(1000),DZ(1000),PTE(1000)
      DIMENSION RXK(1000),RYK(1000),RZK(1000)
C
CCMMON LABELING OF VARIABLES REQUIRED IN OTHER SUBROUTINES
      COMMON/COM1/RX(1000),RY(1000),RZ(1000),LCUT(1000),
     1LL,LD,ITYPE,NVAC
      COMMON/COM2/IH1(20),IH2(8),IHS(10),IHB(6),IHT(6),
     1TARGET(4),TMAS,BULLET(4),BMAS,PLANE,TEMP,THERM
      COMMON/COM3/RXI(1000),RYI(1000),RZI(1000),CVR,EVR,
     1NT,TIME,DT,DTI,ILAY
      COMMON/COM4/IX,IY,IZ,SCX,SCY,SCZ,IDEEP,D1X,D1Y,D1Z
      COMMON/COM5/ROE,ROE2,ROEM,EXA,EXB,PEXA,PEXB,FXA,PFXA,
     1IQ,TSAVE,BSAVE
      COMMON/COM6/FX(1000),FY(1000),FZ(1000),PAC,PFPTC,FM
      COMMON/COM7/PPTC,TPOT,PPE(1000),TLPE,ROEL,ROEL2,NEW
      COMMON/COM8/ROEA,ROEB,ROEC,ROEC2,CP0,CP1,CP2,CP3,
     1CF0,CF1,CF2,CGD1,CGD2,CGB1,CGB2,CGF1,CGF2
      COMMON/COMA/ A(4,5),MCRO
C
READ STATEMENT FORMATS
 9010 FORMAT(20A4)
 9020 FORMAT(8A4,3F8.5,2F5.2)
 9030 FORMAT(4A4,3F8.5,6A4,F6.2)
 9040 FORMAT(F6.2,F5.3,I5,6I4,3F5.2,I2)
 9050 FORMAT(10A4,A4,4I3,F8.4,I4)
C
WRITE STATEMENT FORMATS
 9610 FORMAT(1H1)
 9620 FORMAT(47X,'SUMMARY OF ATOMS'//,35X,8A4,', NT ='I4,//,
     13(' ATOM        POSITION         BIND ENERGY    '),//)
 9630 FORMAT(3(I5,3F6.2,F8.4,8X))
 9640 FORMAT(/4X,F10.3,25H EV,TOTAL KINETIC ENERGY,,F10.3,
     127H EV,TOTAL POTENTIAL ENERGY,F10.3,13H EV,REDUCTION,
     1//,20X,F10.3,50HEV, LOCAL POTENTIAL ENERGY, IN VOLUME
     1OF RADIUS = ,F5.2, /30X, 16HCHANGE IN TLPE =, F10.3)
 9650 FORMAT(105X,4HPAGE,I3,/,1H1)
 9660 FORMAT(/ '      ATOM     DX          DY          DZ
     1VX          VY          VZ          KE          PE          TE'/)
 9670 FORMAT(1I8,3F10.3,3F10.1,3F10.4 )
C
INITIALIZING
      START=0.01*ITIME(XX)
      DO 2 I=1,1000
      LCUT(I)=0
      RXK(I)=0.0
      RYK(I)=0.0
      RZK(I)=0.0
      VX(I)=0.0
      VY(I)=0.0
      VZ(I)=0.0
      PKE(I)=0.0
      PPE(I)=0.0
      PTE(I)=0.0
      RX(I)=0.0
      RY(I)=0.0
      RZ(I)=0.0
      FX(I)=0.0
      FY(I)=0.0
      FZ(I)=0.0
      RXI(I)=0.0
      RYI(I)=0.0
```

```
    2 RZI(I)=0.0
      ISHUT=1
      NRUN=0
C
INPUT DATA
       READ ( 5,9010) IH1
       READ ( 5,9020) IH2,DCON,ALPHA,RE,ROEC,ROEL
       READ ( 5,9030) BULLET,BMAS,PEXA,PEXB,IHB,THERM
       READ ( 5,9030) TARGET,TMAS,EXA,EXB,IHT,TEMP
       READ ( 5,9040) EVR,DTI,NTT,NS,ND,IP,IDEEP,ITYPE,NVAC,
     1D1X,D1Y,D1Z,IQ
       READ ( 5,9050) IHS,PLANE,LS,IX,IY,IZ,CVR,MCRO
C
CONSTANTS AND SCALING FACTORS
      ROE2=3.0
      ROE=SQRT(ROE2)
      ROEM = ROE-DTI
      ROEL2=ROEL*ROEL
      CVE=1.60E-19
      EV=EVR*1.0E+3
      CVM=1.672E-27
      FM=1.0E-10
      FM2=FM*FM
      CVD=CVR*1.0E-10
      CVED=CVE/CVD
      PTMAS=TMAS*CVM
      PBMAS=BMAS*CVM
      HTMAS=0.5*PTMAS/CVE
      HBMAS=0.5*PBMAS/CVE
      TSAVE=BMAS/(BMAS+TMAS)
      BSAVE=TMAS/(BMAS+TMAS)
C
REPULSIVE POTENTIAL PARAMETERS
      FXA=ALOG(-EXB*CVED)+EXA
      PFXA=ALOG(-PEXB*CVED)+PEXA
      PPTC=EXP(PEXA+PEXB*ROE)
      PAC=ALOG(CVED)+PEXA
      PFPTC=EXP(PAC+PEXB*ROE)
C
ATTRACTIVE POTENTIAL PARAMETERS
      CGD1=ALOG(DCON)+2.0*ALPHA*RE
      CGD2=ALOG(2.0*DCON)+ALPHA*RE
      CGB1=-2.0*ALPHA*CVR
      CGB2=-ALPHA*CVR
      CGF1=ALOG(-CGB1*CVED)+CGD1
      CGF2=ALOG(-CGB2*CVED)+CGD2
C
CUTOFF DISTANCES FOR ATTRACTIVE AND REPULSIVE POTENTIALS
      ROEA=1.50/CVR
      ROEB=2.0/CVR
      ROEC2=ROEC*ROEC
C
PARAMETERS FOR CALCULATION OF THE BEST CUBIC FIT IN THE GAP
BETWEEN MAXIMUM DISTANCE CUTOFF OF THE REPULSIVE POTENTIAL
(ROEA), AND MINIMUM DISTANCE CUTOFF OF THE ATTRACTIVE POTEN-
TIAL (ROEB).  SUBROUTINE CROSYM ACTUALLY PERFORMS THIS CURVE
FITTING.
      A(1,1)=1.0
      A(1,2)=ROEA
      A(1,3)=ROEA*ROEA
      A(1,4)=ROEA**3
      A(1,5)=EXP(EXA+EXB*ROEA)
      A(2,1)=1.0
      A(2,2)=ROEB
      A(2,3)=ROEB*ROEB
      A(2,4)=ROEB**3
      A(2,5)=EXP(CGD1+CGB1*ROEB)-EXP(CGD2+CGB2*ROEB)
      A(3,1)=0.0
      A(3,2)=-1.0
      A(3,3)=-2.0*ROEA
      A(3,4)=-3.0*ROEA*ROEA
      A(3,5)=EXP(FXA+EXB*ROEA)/CVED
```

```
      A(4,1)=0.0
      A(4,2)=-1.0
      A(4,3)=-2.0*ROEB
      A(4,4)=-3.0*ROEB*ROEB
      A(4,5)=(EXP(CGF1+CGB1*ROEB)-EXP(CGF2+CGB2*ROEB))/CVED
      CALL CROSYM
      CP0=A(1,5)
      CP1=A(2,5)
      CP2=A(3,5)
      CP3=A(4,5)
      CF0=-CP1*CVED
      CF1=-2.0*CP2*CVED
      CF2=-3.0*CP3*CVED
C
SELECTION OF THE DESIRED CRYSTAL STRUCTURE AND ORIENTATION.
100, 110, AND 111 PLANES OF FACE-CENTERED, BODY-CENTERED,
AND DIAMOND STRUCTURES ARE ALLOWED.  ILAY AND IDEEP ARE VAR-
IABLES ESTABLISHING THE NUMBER OF MOBILE LAYERS IN THE
CRYSTAL.  RXI(I) AND RXK(I) ARE VARIABLES SAVING THE ORIGIN-
AL X-POSITION OF THE I'TH ATOM.  Y AND Z POSITIONS ARE
ANALOGOUS.
      GO TO ( 11,12,13,14,15,16,17,18,19),LS
   11 CALL L100
      GO TO 30
   12 CALL L110
      GO TO 30
   13 CALL L111
      GO TO 30
   14 CALL B100
      GO TO 30
   15 CALL B110
      GO TO 30
   16 CALL B111
      GO TO 30
   17 CALL D100
      GO TO 30
   18 CALL D110
      GO TO 30
   19 CALL D111
   30 ILAY=IDEEP
      IF(IDEEP) 35,35,40
   35 LD=LL
      ILAY=IY
   40 DO 45 I=1,LL
      RXK(I)=RX(I)
      RYK(I)=RY(I)
      RZK(I)=RZ(I)
      RXI(I)=RX(I)
      RYI(I)=RY(I)
   45 RZI(I)=RZ(I)
C
THIS SECTION ALLOWS ONE TO REPEAT A RUN OF THE PROGRAM WITH
DIFFERENT DATA WITHOUT REPEATING INITIALIZATION, POTENTIAL
PARAMETER CALCULATIONS AND CRYSTAL LATTICE BUILDING.  SUB-
ROUTINE PLACE USES LCUT(I) AND NVAC TO CREATE VACANCIES,
INTERSTITIALS, AND REPLACEMENT IMPURITIES AT DESIRED LOCA-
TIONS IN THE LATTICE.
      IF(NRUN.EQ.0) GO TO 60
   50  READ ( 5,9040) EVR,DTI,NTT,NS,ND,IP,IDEEP,ITYPE,NVAC,
     1DIX,DIY,DIZ,IQ
      IF(DTI.EQ.0) GO TO 9999
      DO 55 I=1,LL
      LCUT(I)=0
      RX(I)=RXI(I)
      RY(I)=RYI(I)
      RZ(I)=RZI(I)
      RXK(I)=RXI(I)
      RYK(I)=RYI(I)
   55 RZK(I)=RZI(I)
   60 NRUN=1
      CALL PLACE
      RXI(1)=RX(1)
```

```
      RYI(1)=RY(1)
      RZI(1)=RZ(1)
      RXK(1)=RX(1)
      RYK(1)=RY(1)
      RZK(1)=RZ(1)
      DO 65 I=1,LL
      VX(I)=0.0
      VY(I)=0.0
      VZ(I)=0.0
      PPE(I)=0.0
      PKE(I)=0.0
   65 PTE(I)=0.0
      TPOT=0.0
      NEW=0
C
THE ENERGY SUBROUTINE CALCULATES THE POTENTIAL ENERGY OF
EACH ATOM IN THE LATTICE.  SUBROUTINE LOCAL SUMS UP THIS
ENERGY FOR ALL ATOMS WITHIN A SPECIFIC RADIUS OF THE POINT
DEFECT.
      CALL ENERGY
      CALL LOCAL
      BIND=-TPOT
      TPKE=0.0
      TLPEO=TLPE
      DLPE=TLPE-TLPEO
      TE=TPOT+BIND
C
THIS SECTION PRINTS OUT X, Y, AND Z COORDINATES, IN LATTICE
UNITS, AND BINDING ENERGIES OF EACH ATOM IN THE CRYSTAL AT
TIME ZERO.
      TIME=0.0
      NT=0
       WRITE ( 6,9610)
       WRITE ( 6,9620) IH2,NT
      DO 70 I=1,LL,3
      K=I+1
      J=I+2
   70  WRITE ( 6,9630) I,RX(I),RY(I),RZ(I),PPE(I),K,RX(K),
     1RY(K),RZ(K),PPE(K),J,RX(J),RY(J),RZ(J),PPE(J)
       WRITE ( 6,9640) TPKE,TPOT,TE,TLPE,ROEL,DLPE
      NPAGE=1
      NPAGE=NPAGE+1
       WRITE ( 6,9650) NPAGE
C
THIS IS THE MAIN BODY OF THE PROGRAM.  BY USE OF THE AVERAGE
FORCE METHOD, EXPLAINED IN DETAIL IN APPENDIX C, IT DOES ALL
THE DYNAMICS FOR EACH INDIVIDUAL ATOM.  SUBROUTINE STEP
CALCULATES ALL MUTUAL FORCES AMONG THE ATOMS.  BASED ON THE
FORCES, THIS SECTION THEN CALCULATES TEMPORARY POSITIONS FOR
THE PRIMARY, AND ALL OTHER ATOMS; RECALCULATES FORCES IN
STEP; AND THEN RECALCULATES FINAL POSITIONS FOR THE PRIMARY
AND ALL OTHER ATOMS, BASED ON THE AVERAGE OF THESE TWO
FORCES.  THIS SECTION ALSO INCLUDES ALL KINETIC ENERGY CAL-
CULATIONS, BASED ON THE VELOCITIES INVOLVED; AND FINALLY
CALCULATES A NEW TIMESTEP DURATION FOR USE IN THE NEXT TIME-
STEP, BASED ON EITHER A MAXIMUM ALLOWED FORCE, OR MAXIMUM
ALLOWED ENERGY.  (SEE APP. C)  VELOCITIES ARE HALVED AT THE
END OF EACH TIMESTEP AS A METHOD OF DAMPING.
   95 TFAC=2.0*PTMAS*DTI*CVD
      TFACB=2.0*PBMAS*DTI*CVD
      DT=1.0E-14
  100 DTOD=DT/CVD
      HDTOD=0.5*DTOD
      DTOM=DT/PTMAS
      HDTOM=0.5*DTOM
      DTOMB=DT/PBMAS
      HDTOMB=0.5*DTOMB
  200 CALL STEP
      IF(LCUT(1).GT.0) GO TO 240
      I=1
      RXK(I)=RX(I)
      RYK(I)=RY(I)
```

```
      RZK(I)=RZ(I)
      RX(I)=RX(I)+DTOD*(HDTOMB*FX(I)+VX(I))
      RY(I)=RY(I)+DTOD*(HDTOMB*FY(I)+VY(I))
      RZ(I)=RZ(I)+DTOD*(HDTOMB*FZ(I)+VZ(I))
240   DO 245 I=2,LD
      IF(LCUT(I).GT.0)GO TO 245
      RXK(I)=RX(I)
      RYK(I)=RY(I)
      RZK(I)=RZ(I)
      RX(I)=RX(I)+DTOD*(HDTOM*FX(I)+VX(I))
      RY(I)=RY(I)+DTOD*(HDTOM*FY(I)+VY(I))
      RZ(I)=RZ(I)+DTOD*(HDTOM*FZ(I)+VZ(I))
245   CONTINUE
      CALL STEP
      EMAX=0.0
      FMAX=0.0
      TIME=TIME+DT
      NT=NT+1
      IF(LCUT(1).GT.0) GO TO 265
      I=1
      VSS=VX(I)
      VX(I)=VSS+HDTOMB*FX(I)
      RX(I)=RXK(I)+(VX(I)+VSS)*HDTOD
      VSS=VY(I)
      VY(I)=VSS+HDTOMB*FY(I)
      RY(I)=RYK(I)+(VY(I)+VSS)*HDTOD
      VSS=VZ(I)
      VZ(I)=VSS+HDTOMB*FZ(I)
      RZ(I)=RZK(I)+(VZ(I)+VSS)*HDTOD
      PKE(I)=VX(I)*VX(I)+VY(I)*VY(I)+VZ(I)*VZ(I)
      EMAX=PKE(I)
      FMAX=FX(I)*FX(I)+FY(I)*FY(I)+FZ(I)*FZ(I)
      FORC1=FMAX
260   FX(I)=0.0
      FY(I)=0.0
      FZ(I)=0.0
265   DO 280 I=2,LD
      IF(LCUT(I).GT.0)GO TO 280
      VSS=VX(I)
      VX(I)=VSS+HDTOM*FX(I)
      RX(I)=RXK(I)+(VX(I)+VSS)*HDTOD
      VSS=VY(I)
      VY(I)=VSS+HDTOM*FY(I)
      RY(I)=RYK(I)+(VY(I)+VSS)*HDTOD
      VSS=VZ(I)
      VZ(I)=VSS+HDTOM*FZ(I)
      RZ(I)=RZK(I)+(VZ(I)+VSS)*HDTOD
      PKE(I)=VX(I)*VX(I)+VY(I)*VY(I)+VZ(I)*VZ(I)
275   F2=FX(I)*FX(I)+FY(I)*FY(I)+FZ(I)*FZ(I)
      FX(I)=0.0
      FY(I)=0.0
      FZ(I)=0.0
      IF(F2.GT.FMAX) FMAX=F2
      IF(PKE(I).GT.EMAX) EMAX=PKE(I)
280   CONTINUE
      IF(EMAX.EQ.0.0) GO TO 285
      IF(FMAX.EQ.0.0) GO TO 285
      GO TO 287
285   DT=1.0E-14
      GO TO 300
287   IF(EMAX.EQ.PKE(1)) GO TO 290
      IF(FMAX.EQ.FORC1) GO TO 290
      EMAX=SQRT(EMAX)
      FMAX=SQRT(FMAX)
      DT=SQRT(TFAC/FMAX)
      FTERM=FMAX*DT/(2.0*PTMAS)
      GO TO 295
290   EMAX=SQRT(PKE(1))
      FMAX=SQRT(FORC1)
      IF(FORC1.EQ.0.0) GO TO 285
      DT=SQRT(TFACB/FMAX)
      FTERM=FMAX*DT/(2.0*PBMAS)
```

```
  295 IF(EMAX.LE.FTERM) GO TO 300
      FDTI=DTI*CVD
      DT=FDTI/EMAX
  300 IF(ISHUT.EQ.-1) GO TO 400
  310 IF(NS-NT) 400,400,320
  320 DO 325 I=1,LL
      VX(I)=0.5*VX(I)
      VY(I)=0.5*VY(I)
  325 VZ(I)=0.5*VZ(I)
      GO TO 100
  340 DO 350 I=1,LL
      RX(I)=RXK(I)
      RY(I)=RYK(I)
  350 RZ(I)=RZK(I)
      NTT=NT
C
THE PRINT SUBROUTINE PLACES A HEADING OF PERTINENT INFORMA-
TION AT THE TOP OF EACH TIMESTEP PRINTOUT.
  400 CALL PRINT
C
POTENTIAL ENERGY AND LOCAL POTENTIAL ENERGY FOR EACH ATOM
ARE CALCULATED BASED ON THE NEW POSITIONS.  SUMMATIONS OF
TOTAL POTENTIAL AND KINETIC ENERGY FOR THE LATTICE ARE PER-
FORMED.  DX, DY, AND DZ KEEP TRACK OF MOTION RELATIVE TO THE
INITIAL POSITION AT TIME ZERO FOR EACH ATOM.
  410 TPOT=0.0
      DO 450 I=1,LL
      PPE(I)=0.0
  450 PTE(I)=0.0
      CALL ENERGY
      CALL LOCAL
      DLPE=TLPE-TLPEO
      PKE(1)=HBMAS*PKE(1)
      TPKE=PKE(1)
      PTE(1)=PKE(1)+PPE(1)
      DO 620 I=2,LL
      PKE(I)=HTMAS*PKE(I)
      TPKE=TPKE+PKE(I)
  620 PTE(I)=PKE(I)+PPE(I)
      TE=TPOT+BIND
       WRITE ( 6,9660)
  700 DO 750 I=1,LD
      DX(I)=RX(I)-RXI(I)
      DY(I)=RY(I)-RYI(I)
      DZ(I)=RZ(I)-RZI(I)
C
THIS SECTION PRINTS THE RELATIVE MOTION, VELOCITY, AND
ENERGY OF EACH ATOM, FOR EVERY TIMESTEP SO DESIGNATED:  IE,
EVERY ND'TH TIMESTEP, BEGINNING WITH #NS AND ENDING WITH
#NTT.
  720  WRITE ( 6,9670) I,DX(I),DY(I),DZ(I),VX(I),VY(I),
     1VZ(I),PKE(I),PPE(I),PTE(I)
  750 CONTINUE
       WRITE ( 6,9640) TPKE,TPOT,TE,TLPE,ROEL,DLPE
       WRITE ( 6,9650) NPAGE
      NPAGE=NPAGE+1
      IF(NT-NTT) 760,950,950
  760 DO 780 I=1,LL
      VX(I)=0.5*VX(I)
      VY(I)=0.5*VY(I)
      VZ(I)=0.5*VZ(I)
  780 CONTINUE
  790 NS=NS+ND
      GO TO 100
  950 CONTINUE
C
THIS SECTION PRINTS OUT X, Y, AND Z COORDINATES AND BINDING
ENERGIES OF EACH ATOM IN THE CRYSTAL AT THE END OF THE
PROGRAM.
  955  WRITE ( 6,9620) IH2,NT
      DO 965 I=1,LL,3
      K=I+1
```

```
      J=I+2
  965  WRITE ( 6,9630) I,RX(I),RY(I),RZ(I),PPE(I),K,RX(K),
     1RY(K),RZ(K),PPE(K),J,RX(J),RY(J),RZ(J),PPE(J)
       WRITE ( 6,9640) TPKE,TPOT,TE,TLPE,RCEL,DLPE
       WRITE ( 6,9650) NPAGE
 1000 IF(ISHUT) 9999,50,50
 9999 STOP
      END

      SUBROUTINE CROSYM
C
SOLVES M SIMULTANEOUS EQUATIONS BY THE METHOD OF CROUT
THIS SUBROUTINE FITS THE BEST CUBIC BETWEEN THE REPULSIVE
AND ATTRACTIVE PARTS OF THE POTENTIAL.
C
      COMMON/COMA/ A(4,5),MCRO
      M=MCRO
      N=M+1
      I1=1
  100 I3=I1
      SUM=ABS(A(I1,I1))
      DO 120 I=I1,M
      IF(SUM-ABS(A(I,I1))) 110,120,120
  110 I3=I
      SUM=ABS(A(I,I1))
  120 CONTINUE
      IF(I3-I1) 130,150,130
  130 DO 140 J=1,N
      SUM=-A(I1,J)
      A(I1,J)=A(I3,J)
  140 A(I3,J)=SUM
  150 I3=I1+1
      DO 160 I=I3,M
  160 A(I,I1)=A(I,I1)/A(I1,I1)
  170 J2=I1-1
      I3=I1+1
      IF(J2) 180,200,180
  180 DO 190 J=I3,N
      DO 190 I=1,J2
  190 A(I1,J)=A(I1,J)-A(I1,I)*A(I,J)
      IF(I1-M) 200,220,200
  200 J2=I1
      I1=I1+1
      DO 210 I=I1,M
      DO 210 J=1,J2
  210 A(I,I1)=A(I,I1)-A(I,J)*A(J,I1)
      IF(I1-M) 100,170,100
  220 DO 240 I=1,M
      J2=M-I
      I3=J2+1
      A(I3,N)=A(I3,N)/A(I3,I3)
      IF(J2) 230,250,230
  230 DO 240 J=1,J2
  240 A(J,N)=A(J,N)-A(I3,N)*A(J,I3)
  250 RETURN
      END

      SUBROUTINE L100
C
THIS IS A LATTICE GENERATOR FOR THE FCC (100) ORIENTATION.
THE CRYSTAL IS DEVELOPED IN THE ORDER, Z FOLLOWED BY Y,
FOLLOWED BY X.
IT CONTAINS A NONSTANDARD USE OF THE SURFACE RELAXATION
PARAMETER.
C
      COMMON/COM1/RX(1000),RY(1000),RZ(1000),LCUT(1000),
     1LL,LD,ITYPE,NVAC
      COMMON/COM4/IX,IY,IZ,SCX,SCY,SCZ,IDEEP,D1X,D1Y,D1Z
      DIMENSION YLAX(20)
      DATA YLAX/20*0.0/
```

```
      YLAX(1)=-0.097
      YLAX(2)=-0.024
      SCX=1.0
      SCY=1.0
      SCZ=1.0
      M=2
      JT=0
      Y=-SCY
      DO 60 J=1,IY
      Y=Y+SCY
      KT=0
      Z=-SCZ
      DO 59 K=1,IZ
      Z=Z+SCZ
      IT=0
      X=-SCX
      DO 58 I=1,IX
      X=X+SCX
      ITT=IT+JT+KT
      IF(ITT-(ITT/2)*2) 57,30,57
   30 RX(M)=X
      RY(M)=Y+YLAX(J)
      RZ(M)=Z
      M=M+1
   57 CONTINUE
      IT =IT+1
   58 CONTINUE
      KT=KT+1
   59 CONTINUE
      JT = JT + 1
      IF(IDEEP-JT) 60,110,60
   60 CONTINUE
      LL=M-1
  100 RETURN
  110 LD=M-1
      GO TO 60
      END

      SUBROUTINE L110
C
THIS IS A LATTICE GENERATOR FOR THE FCC (110) ORIENTATION.
THE CRYSTAL IS DEVELOPED IN THE ORDER, Z FOLLOWED BY Y,
FOLLOWED BY X.
IT CONTAINS A NONSTANDARD USE OF THE SURFACE RELAXATION
PARAMETER.
C
      COMMON/COM1/RX(1000),RY(1000),RZ(1000),LCUT(1000),
     1LL,LD,ITYPE,NVAC
      COMMON/COM4/IX,IY,IZ,SCX,SCY,SCZ,IDEEP,D1X,D1Y,D1Z
      DIMENSION YLAX(20)
      DATA YLAX/20*0.0/
      YLAX(1)=-0.07
      YLAX(2)=-0.02
      RO=1.0/SQRT(2.0)
      SCX=RO
      SCY=RO
      SCZ=1.0
      M=2
      JT=0
      Y=-SCY
      DO 60 J=1,IY
      Y=Y+SCY
      KT=0
      Z=-SCZ
      DO 59 K=1,IZ
      Z=Z+SCZ
      IT=0
      X=-SCX
      DO 58 I=1,IX
      X=X+SCX
      IF(IT-(IT/2)*2) 21,11,21
```

```
   11 IF(JT-(JT/2)*2) 57,12,57
   12 IF(KT-(KT/2)*2) 57,30,57
   21 IF(JT-(JT/2)*2) 22,57,22
   22 IF(KT-(KT/2)*2) 30,57,30
   30 RX(M)=X
      RY(M)=Y+YLAX(J)
      RZ(M)=Z
      M=M+1
   57 CONTINUE
      IT =IT+1
   58 CONTINUE
      KT=KT+1
   59 CONTINUE
      JT = JT + 1
      IF(IDEEP-JT) 60,110,60
   60 CONTINUE
      LL=M-1
  100 RETURN
  110 LD=M-1
      GO TO 60
      END

      SUBROUTINE L111
C
THIS IS A LATTICE GENERATOR FOR THE FCC (111) ORIENTATION.
THE CRYSTAL IS DEVELOPED IN THE ORDER, Z FOLLOWED BY Y,
FOLLOWED BY X.
IT CONTAINS A NONSTANDARD USE OF THE SURFACE RELAXATION
PARAMETER.
C
      COMMON/CCM1/RX(1000),RY(1000),RZ(1000),LCUT(1000),
     1LL,LD,ITYPE,NVAC
      COMMON/COM4/IX,IY,IZ,SCX,SCY,SCZ,IDEEP,D1X,D1Y,D1Z
      DIMENSION YLAX(20)
      DATA YLAX/20*0.0/
      YLAX(1)=-0.04
      YLAX(2)=-0.01
      SCX=1.0/SQRT(2.0)
      SCY=2.0/SQRT(3.0)
      SCZ=SQRT(1.5)
      SSCZ=SCZ/3.0
      M=2
      JT=0
      Y=-SCY
      DO 60 J=1,IY
      Y=Y+SCY
      JTS=JT+JT/3
      Z=-SCZ
      KT=0
      DO 59 K=1,IZ
      Z=Z+SCZ
      IT=0
      X=-SCX
      DO 58 I=1,IX
      X=X+SCX
      IN=IT+JTS+KT
      IF(IN-(IN/2)*2) 57,30,57
   30 RX(M)=X
      RY(M)=Y+YLAX(J)
      IF(JT-3*(JT/3)) 41,45,41
   41 JTT=JT
   42 JTT=JTT-3
      IF(JTT) 43,45,42
   43 JTT=JTT+3
      ZP=JTT
      RZ(M)=Z+ZP*SSCZ
      GO TO 50
   45 RZ(M)=Z
   50 M=M+1
   57 CONTINUE
      IT=IT+1
```

```
   58 CONTINUE
      KT=KT+1
   59 CONTINUE
      JT=JT+1
      IF(IDEEP-JT) 60,110,60
   60 CONTINUE
      LL=M-1
  100 RETURN
  110 LD=M-1
      GO TO 60
      END

      SUBROUTINE B100
C
THIS IS A LATTICE GENERATOR THE THE BCC (100) ORIENTATION.
THE CRYSTAL IS DEVELOPED IN THE ORDER, X FOLLOWED BY Z,
FOLLOWED BY Y.
IT CONTAINS A NONSTANDARD USE OF THE SURFACE RELAXATION
PARAMETER.
C
      COMMON/COM1/RX(1000),RY(1000),RZ(1000),LCUT(1000),
     1LL,LD,ITYPE,NVAC
      COMMON/COM4/IX,IY,IZ,SCX,SCY,SCZ,IDEEP,D1X,D1Y,D1Z
      DIMENSION YLAX(20)
      DATA YLAX/20*0.0/
      YLAX(1)=-0.20
      YLAX(2)=-0.03
      SCX=1.0
      SCY=1.0
      SCZ=1.0
      M = 2
      JT=0
      Y=-SCY
      DO 60 J=1,IY
      Y=Y+SCY
      KT=0
      Z=-SCZ
      DO 59 K=1,IZ
      Z=Z+SCZ
      IT=0
      X=-SCX
      DO 58 I=1,IX
      X=X+SCX
      IF(IT-(IT/2)*2) 21,11,21
   11 IF(JT-(JT/2)*2) 57,12,57
   12 IF(KT-(KT/2)*2) 57,30,57
   21 IF(JT-(JT/2)*2) 22,57,22
   22 IF(KT-(KT/2)*2) 30,57,30
   30 RX(M)=X
      RY(M)=Y+YLAX(J)
      RZ(M)=Z
      M=M+1
   57 IT=IT+1
   58 CONTINUE
      KT=KT+1
   59 CONTINUE
      JT = JT + 1
      IF(IDEEP-JT) 60,110,60
   60 CONTINUE
      LL=M-1
  100 RETURN
  110 LD=M-1
      GO TO 60
      END
```

```
      SUBROUTINE B110
C
THIS IS A LATTICE GENERATOR THE THE BCC (110) ORIENTATION.
THE CRYSTAL IS DEVELOPED IN THE ORDER, X FOLLOWED BY Z,
FOLLOWED BY Y.
IT CONTAINS A NONSTANDARD USE OF THE SURFACE RELAXATION
PARAMETER.
C
      COMMON/CCM1/RX(1000),RY(1000),RZ(1000),LCUT(1000),
     1LL,LD,ITYPE,NVAC
      COMMON/COM4/IX,IY,IZ,SCX,SCY,SCZ,IDEEP,D1X,D1Y,D1Z
      DIMENSION YLAX(20)
      DATA YLAX/20*0.0/
      YLAX(1)=-0.10
      YLAX(2)=-0.01
      SCX = SQRT(2.0)
      SCY = SQRT(2.0)
      SCZ=1.0
      M=2
      JT=0
      Y=-SCY
      DO 60 J=1,IY
      Y=Y+SCY
      KT=0
      Z=-SCZ
      DO 59 K=1,IZ
      Z=Z+SCZ
      IT=0
      X=-SCX
      DO 58 I=1,IX
      X=X+SCX
      ITT=IT+JT+KT
      IF(ITT-(ITT/2)*2) 57,30,57
   30 RX(M)=X
      RY(M)=Y+YLAX(J)
      RZ(M)=Z
      M = M+1
   57 CONTINUE
      IT =IT+1
   58 CONTINUE
      KT=KT+1
   59 CONTINUE
      JT = JT + 1
      IF(IDEEP-JT) 60,110,60
   60 CONTINUE
      LL=M-1
      RETURN
  110 LD = M-1
      GO TO 60
      END


      SUBROUTINE B111
C
THIS IS A LATTICE GENERATOR FOR THE BCC (111) ORIENTATION.
THE CRYSTAL IS DEVELOPED IN THE ORDER, X FOLLOWED BY Z,
FOLLOWED BY Y.
IT CONTAINS A NONSTANDARD USE OF THE SURFACE RELAXATION
PARAMETER.
C
      COMMON/CCM1/RX(1000),RY(1000),RZ(1000),LCUT(1000),
     1LL,LD,ITYPE,NVAC
      COMMON/COM4/IX,IY,IZ,SCX,SCY,SCZ,IDEEP,D1X,D1Y,D1Z
      DIMENSION YLAX(20)
      DATA YLAX/20*0.0/
      YLAX(1)=-0.10
      YLAX(2)=-0.01
      SCX = SQRT(2.0)
```

```
      SCY = SQRT(1.0/3.0)
      SCZ = SQRT(6.0)
      M = 2
      JT=0
      Y=-SCY
      DO 60 J=1,IY
      Y=Y+SCY
      KT = 0
      JJ = J-(JT/3)*3
      GO TO (5,10,15),JJ
    5 Z =-SCZ
      GO TO 20
   10 Z =-SCZ+SCZ/3.0
      GO TO 20
   15 Z =-SCZ+(2.0*SCZ/3.0)
   20 DO 59 K=1,IZ
      Z=Z+SCZ
      IT = 0
      X=-SCX
      DO 58 I=1,IX
      X=X+SCX
      ITT=IT+JJ+KT-1
      IF(ITT-(ITT/2)*2) 57,30,57
   30 RX(M)=X
      RY(M)=Y+YLAX(J)
      RZ(M)=Z
      M = M+1
   57 IT=IT+1
   58 CONTINUE
      KT=KT+1
   59 CONTINUE
      JT = JT + 1
      IF(IDEEP-JT) 60,110,60
   60 CONTINUE
      LL=M-1
      RETURN
  110 LD=M-1
      GO TO 60
      END

      SUBROUTINE D100
      COMMON/COM1/RX(1000),RY(1000),RZ(1000),LCUT(1000),
     1LL,LD,ITYPE,NVAC
      COMMON/COM4/IX,IY,IZ,SCX,SCY,SCZ,IDEEP,D1X,D1Y,D1Z
      RETURN
      END

      SUBROUTINE D110
      COMMON/COM1/RX(1000),RY(1000),RZ(1000),LCUT(1000),
     1LL,LD,ITYPE,NVAC
      COMMON/COM4/IX,IY,IZ,SCX,SCY,SCZ,IDEEP,D1X,D1Y,D1Z
      RETURN
      END

      SUBROUTINE D111
      COMMON/COM1/RX(1000),RY(1000),RZ(1000),LCUT(1000),
     1LL,LD,ITYPE,NVAC
      COMMON/COM4/IX,IY,IZ,SCX,SCY,SCZ,IDEEP,D1X,D1Y,D1Z
      RETURN
      END

      SUBROUTINE PLACE
C
THIS SUBROUTINE LOCATES A VACANCY, INTERSTITIAL, OR REPLACE-
MENT IMPURITY IN THE LATTICE.
C
      COMMON/COM1/RX(1000),RY(1000),RZ(1000),LCUT(1000),
     1LL,LD,ITYPE,NVAC
```

```
      COMMON/COM4/IX,IY,IZ,SCX,SCY,SCZ,IDEEP,D1X,D1Y,D1Z
      GO TO  (10,20,30), ITYPE
   10 LCUT(NVAC) = 1
      LCUT(1) = 1
      RX(1)=0.0
      RY(1)=0.0
      RZ(1)=0.0
      GO TO 40
   20 RX(1) = RX(NVAC) - D1X
      RY(1) = RY(NVAC) - D1Y
      RZ(1) = RZ(NVAC) + D1Z
      GO TO 40
   30 LCUT(NVAC) = 1
      RX(1) = RX(NVAC)
      RY(1) = RY(NVAC)
      RZ(1) = RZ(NVAC)
   40 RETURN
      END


      SUBROUTINE STEP
C
THIS SUBROUTINE DOES THE DYNAMICS FOR ONE TIMESTEP.
THE FIRST HALF DOES THE DYNAMICS FOR ATOM #1; THE SECOND
HALF FOR ALL OTHERS.
C
      COMMON/COM1/RX(1000),RY(1000),RZ(1000),LCUT(1000),
     1LL,LD,ITYPE,NVAC
      COMMON/COM5/ROE,ROE2,ROEM,EXA,EXB,PEXA,PEXB,FXA,PFXA,
     1IQ,TSAVE,BSAVE
      COMMON/COM6/FX(1000),FY(1000),FZ(1000),PAC,PFPTC,FM
      COMMON/COM8/ROEA,ROEB,ROEC,ROEC2,CP0,CP1,CP2,CP3,
     1CF0,CF1,CF2,CGD1,CGD2,CGB1,CGB2,CGF1,CGF2
      IF(IQ.EQ.1) GO TO 200
      I=1
      IF(LCUT(I))200,105,200
  105 IP=I+1
      DO 195 J=IP,LL
      IF(LCUT(J)) 195,110,195
  110 DRX=RX(J)-RX(I)
      IF(DRX) 113,117,117
  113 IF(DRX+ROE) 195,195,120
  117 IF(DRX-ROE) 120,195,195
  120 DRY=RY(J)-RY(I)
      IF(DRY) 123,127,127
  123 IF(DRY+ROE) 195,195,130
  127 IF(DRY-ROE) 130,195,195
  130 DRZ=RZ(J)-RZ(I)
      IF(DRZ) 133,137,137
  133 IF(DRZ+ROE) 195,195,140
  137 IF(DRZ-ROE) 140,195,195
  140 DIST=DRX*DRX+DRY*DRY+DRZ*DRZ
      IF(DIST-ROE2) 150,195,195
  150 DIST=SQRT(DIST)
  160 IF(DIST-ROEM) 162,162,165
  162 FORCE=EXP(PFXA+PEXB*DIST)
      GO TO 180
  165 DFF=ROE-DIST
      IF(DFF-1.0E-10) 195,195,167
  167 FORCE=(EXP(PAC+PEXB*DIST)-PFPTC)/DFF
  180 IF(FM-FORCE) 190,190,195
  190 FOD=FORCE/DIST
      FA=FOD*DRX
      FX(J)=FX(J)+FA
      FX(I)=FX(I)-FA
      FA=FOD*DRY
      FY(J)=FY(J)+FA
      FY(I)=FY(I)-FA
      FA=FOD*DRZ
      FZ(J)=FZ(J)+FA
      FZ(I)=FZ(I)-FA
  195 CONTINUE
```

```
C
  200 DO 300 I=IQ,LD
      IF(LCUT(I)) 300,205,300
  205 IP=I+1
      DO 295 J=IP,LL
      IF(LCUT(J)) 295,210,295
  210 DRX=RX(J)-RX(I)
      IF(DRX) 213,217,217
  213 IF(DRX+ROEC) 295,295,220
  217 IF(DRX-ROEC) 220,295,295
  220 DRY=RY(J)-RY(I)
      IF(DRY) 223,227,227
  223 IF(DRY+ROEC) 295,295,230
  227 IF(DRY-ROEC) 230,295,295
  230 DRZ=RZ(J)-RZ(I)
      IF(DRZ) 233,237,237
  233 IF(DRZ+ROEC) 295,295,240
  237 IF(DRZ-ROEC) 240,295,295
  240 DIST=DRX*DRX+DRY*DRY+DRZ*DRZ
      IF(DIST-ROEC2) 250,295,295
  250 DIST=SQRT(DIST)
      IF(DIST-ROEA) 260,255,255
  255 IF(DIST-ROEB) 265,270,270
  260 FORCE=EXP(FXA+EXB*DIST)
      GO TO 280
  265 FORCE=DIST*(DIST*CF2+CF1)+CF0
      GO TO 280
  270 FORCE=EXP(CGF1+CGB1*DIST)-EXP(CGF2+CGB2*DIST)
  280 IF(ABS(FORCE).LE.FM) GO TO 295
      FOD = FORCE/DIST
      FA=FOD*DRX
      FX(J)=FX(J)+FA
      FX(I)=FX(I)-FA
      FA=FOD*DRY
      FY(J)=FY(J)+FA
      FY(I)=FY(I)-FA
      FA=FOD*DRZ
      FZ(J)=FZ(J)+FA
      FZ(I)=FZ(I)-FA
  295 CONTINUE
  300 CONTINUE
      RETURN
      END


      SUBROUTINE ENERGY
C
THIS SUBROUTINE CALCULATES THE MUTUAL POTENTIAL ENERGIES.
THE FIRST HALF DOES THE DYNAMICS FOR ATOM #1; THE SECOND
HALF FOR ALL OTHERS.
C
      COMMON/COM1/RX(1000),RY(1000),RZ(1000),LCUT(1000),
     1LL,LD,ITYPE,NVAC
      COMMON/COM5/ROE,ROE2,ROEM,EXA,EXB,PEXA,PEXB,FXA,PFXA,
     1IQ,TSAVE,BSAVE
      COMMON/COM7/PPTC,TPOT,PPE(1000),TLPE,ROEL,ROEL2,NEW
      COMMON/COM8/ROEA,ROEB,ROEC,ROEC2,CP0,CP1,CP2,CP3,
     1CF0,CF1,CF2,CGD1,CGD2,CGB1,CGB2,CGF1,CGF2
      IF(IQ.EQ.1) GO TO 200
      I=1
      IF(LCUT(I)) 600,505,600
  505 IP=I+1
      DO 595 J=IP,LL
      IF(LCUT(J)) 595,510,595
  510 DRX=RX(J)-RX(I)
      IF(DRX) 513,517,517
  513 IF(DRX+ROE) 595,595,520
  517 IF(DRX-ROE) 520,595,595
  520 DRY=RY(J)-RY(I)
      IF(DRY) 523,527,527
  523 IF(DRY+ROE) 595,595,530
  527 IF(DRY-ROE) 530,595,595
```

```
  530 DRZ=RZ(J)-RZ(I)
      IF(DRZ) 533,537,537
  533 IF(DRZ+ROE) 595,595,540
  537 IF(DRZ-ROE) 540,595,595
  540 DIST=DRX*DRX+DRY*DRY+DRZ*DRZ
      IF(DIST-ROE2) 550,595,595
  550 DIST=SQRT(DIST)
  560 POT=EXP(PEXA+PEXB*DIST)-PPTC
  580 TPOT=TPOT+POT
      PPE(I)=PPE(I)+BSAVE*POT
      PPE(J)=PPE(J)+TSAVE*POT
  595 CONTINUE
  600 CONTINUE
C
  200 DO 300 I=IQ,LL
      IF(LCUT(I)) 300,205,300
  205 IP=I+1
      DO 295 J=IP,LL
      IF(LCUT(J)) 295,210,295
  210 DRX=RX(J)-RX(I)
      IF(DRX) 213,217,217
  213 IF(DRX+ROEC) 295,295,220
  217 IF(DRX-ROEC) 220,295,295
  220 DRY=RY(J)-RY(I)
      IF(DRY) 223,227,227
  223 IF(DRY+ROEC) 295,295,230
  227 IF(DRY-ROEC) 230,295,295
  230 DRZ=RZ(J)-RZ(I)
      IF(DRZ) 233,237,237
  233 IF(DRZ+ROEC) 295,295,240
  237 IF(DRZ-ROEC) 240,295,295
  240 DIST=DRX*DRX+DRY*DRY+DRZ*DRZ
      IF(DIST-ROEC2) 250,295,295
  250 DIST=SQRT(DIST)
      IF(DIST-ROEA) 260,255,255
  255 IF(DIST-ROEB) 265,270,270
  260 POT=EXP(EXA+EXB*DIST)
      GO TO 280
  265 POT=DIST*(DIST*(DIST*CP3+CP2)+CP1)+CP0
      GO TO 280
  270 POT=EXP(CGD1+CGB1*DIST)-EXP(CGD2+CGB2*DIST)
  280 TPOT=TPOT+POT
      SAVE=0.5*POT
      PPE(I)=PPE(I)+SAVE
      PPE(J)=PPE(J)+SAVE
  295 CONTINUE
  300 CONTINUE
      RETURN
      END


      SUBROUTINE LOCAL
C
THIS SUBROUTINE CALCULATES THE TOTAL POTENTIAL ENERGY IN A
SMALL VOLUME AROUND A VACANCY OR INTERSTITIAL.
C
      COMMON/COM1/RX(1000),RY(1000),RZ(1000),LCUT(1000),
     1LL,LD,ITYPE,NVAC
      COMMON/COM7/PPTC,TPOT,PPE(1000),TLPE,ROEL,ROEL2,NEW
      DIMENSION LCCAT(500)
      K=1
      TLPE=0.0
      IF(NEW.EQ.1)GO TO 305
    8 GO TO (10,20,20),ITYPE
   10 I=NVAC
      GO TO 200
   20 I=1
  200 DO 300 J=1,LD
      IF(I.EQ.J) GO TO 250
  210 DRX=RX(J)-RX(I)
      IF(DRX) 213,217,217
  213 IF(DRX+ROEL) 295,295,220
```

```
  217 IF(DRX-ROEL) 220,295,295
  220 DRY=RY(J)-RY(I)
      IF(DRY) 223,227,227
  223 IF(DRY+ROEL) 295,295,230
  227 IF(DRY-ROEL) 230,295,295
  230 DRZ=RZ(J)-RZ(I)
      IF(DRZ) 233,237,237
  233 IF(DRZ+ROEL) 295,295,240
  237 IF(DRZ-ROEL) 240,295,295
  240 DIST=DRX*DRX+DRY*DRY+DRZ*DRZ
      ROEL2=ROEL*ROEL
      IF(DIST-ROEL2) 250,295,295
  250 LOCAT(K)=J
      K=K+1
  295 CONTINUE
  300 CONTINUE
      KF=K-1
  305 DO 310 K=1,KF
      TLPE=TLPE+PPE(LOCAT(K))
  310 CONTINUE
      NEW=1
      RETURN
      END


      SUBROUTINE PRINT .
C
THIS SUBROUTINE PRINTS THE HEADING OF ALL PERTINENT INFORMA-
TION AT THE TOP OF EACH TIMESTEP PRINTOUT.
C
      COMMON/COM1/RX(1000),RY(1000),RZ(1000),LCUT(1000),
     1LL,LD,ITYPE,NVAC
      COMMON/COM2/IH1(20),IH2(8),IHS(10),IHB(6),IHT(6),
     1TARGET(4),TMAS,BULLET(4),BMAS,PLANE,TEMP,THERM
      COMMON/COM3/RXI(1000),RYI(1000),RZI(1000),CVR,EVR,
     1NT,TIME,DT,DTI,ILAY
      COMMON/COM4/IX,IY,IZ,SCX,SCY,SCZ,IDEEP,D1X,D1Y,D1Z
      COMMON/COM5/ROE,ROE2,ROEM,EXA,EXB,PEXA,PEXB,FXA,PFXA,
     1IQ,TSAVE,BSAVE
      COMMON/COM8/ROEA,ROEB,ROEC,ROEC2,CP0,CP1,CP2,CP3,
     1CF0,CF1,CF2,CGD1,CGD2,CGB1,CGB2,CGF1,CGF2
 9710 FORMAT(40X,10A4,/,28X,20A4,/)
 9720 FORMAT(9H TARGET -,4A4,10HPRIMARY - ,4A4,1X,14HLATTICE
     1 UNIT =,F7.4,4H ANG)
 9730 FORMAT(4X,6HMASS =,F7.2,13X,6HMASS =,F7.2,9X,14HLATTIC
     1E TEMP =F5.2,7H DEG K,,18H  THERMAL CUTOFF =,F5.2,3H E
     1V/)
 9740 FORMAT(2H (,A4,8H) PLANE,,18H  PRIMARY ENERGY =,
     1 F5.2,21HKEV,  CRYSTAL SIZE ( ,I2,3H X ,I2,3H X ,I2,3H
     1 ),, 4X, 16HVACANCY IN SITE , I4/)
 9741 FORMAT(2H (,A4,8H) PLANE,,18H  PRIMARY ENERGY =,
     1 F5.2,21HKEV,  CRYSTAL SIZE ( ,I2,3H X ,I2,3H X ,I2,3H
     1 ),, 4X, 15HINTERSTITIAL (-,F5.2,2H,-,F5.2,2H,+,F5.2,
     112H) FROM SITE ,I4/)
 9742 FORMAT(2H (,A4,8H) PLANE,,18H  PRIMARY ENERGY =,
     1 F5.2,21HKEV,  CRYSTAL SIZE ( ,I2,3H X ,I2,3H X ,I2,3H
     1 ),, 4X, 20HREPLACEMENT IN SITE , I4/)
 9750 FORMAT(30H PRIMARY START POINT (LU)  X =,F5.2,5H, Y =,
     1F5.2,5H, Z =,F5.2,5X,I3,' LAYERS ARE FREE TO MOVE',
     110X,4HIQ =,I2/)
 9760 FORMAT(12H POTENTIAL  ,6A4,3X,5HPEXA=,F9.5,2X,5HPEXB=,
     1F9.5,2X,5HPFXA=,F9.5)
 9765 FORMAT(12X,6A4,3X,5HEXA =,F9.5,2X,5HEXB =,F9.5,2X,5HFX
     1A =,F9.5/)
 9770 FORMAT(' WHEN',F8.4,' < R <',F8.4,' THE MATCHING POTEN
     1TIAL PARAMETERS ARE',//,'        CP0 =',F10.3,', CP1 ='
     1F10.3,', CP2 =',F10.3,', CP3 =',F10.3,/,'        CF0 ='
     1E10.3,', CF1 =',E10.3,', CF2 =',E10.3,//)
 9780 FORMAT(' CUT-OFF AT',F5.2,', WHEN R > ',F6.3,' LU, MOR
     1SE POTENTIAL PARAMETERS ARE', 8A4,//,10X,'   CGD1 =',
     1F8.4,', CGD2 =',F8.4,', CGB1 =',F8.4,', CGB2 =',F8.4,
     1', CGF1 =',F8.4,', CGF2 =',F8.4,//)
```

```
9790 FORMAT(10H TIMESTEP ,I4,22X,6HDTI = , F5.3, 5H LU, ,
    122H  ELAPSED TIME (SEC) =, E10.4,21H, LAST TIMESTEP WA
    1S =, E10.4/)
      WRITE ( 6,9710) IHS,IH1
      WRITE ( 6,9720) TARGET,BULLET,CVR
      WRITE ( 6,9730) TMAS,BMAS,TEMP,THERM
     GO TO (401,402,403), ITYPE
 401  WRITE ( 6,9740) PLANE,EVR,IX,IY,IZ,NVAC
     GO TO 405
 402  WRITE ( 6,9741) PLANE,EVR,IX,IY,IZ,D1X,D1Y,D1Z,NVAC
     GO TO 405
 403  WRITE ( 6,9742) PLANE,EVR,IX,IY,IZ,NVAC
 405  WRITE ( 6,9750) RXI(1),RYI(1),RZI(1),ILAY,IQ
      WRITE ( 6,9760) IHB,PEXA,PEXB,PFXA
      WRITE ( 6,9765) IHT,EXA,EXB,FXA
      WRITE ( 6,9770) ROEA,ROEB,CP0,CP1,CP2,CP3,CF0,CF1,CF2
      WRITE ( 6,9780) ROEC,ROEB,IH2,CGD1,CGD2,CGB1,CGB2,
    1CGF1,CGF2
      WRITE ( 6,9790) NT,DTI,TIME,DT
     RETURN
     END
```

BIBLIOGRAPHY

1. Gay, W.L., Harrison, D.E. Jr., "Machine Simulation of Collisions Between a Copper Atom and a Copper Lattice", The Physical Review, V. 135, No. 6A, p A1780-A1790, 14 Sept 1964.

2. Harrison, D.E. Jr., Levy, N.S., Johnson, J.P. III, and Effron, H.M., "Computer Simulation of Sputtering", Journal of Applied Physics, V. 39, No. 8, p 3742-3761, July 1968.

3. Harrison, D.E., Jr., "Additional Information on Computer Simulation of Sputtering", Journal of Applied Physics, V. 40, No. 9, p 3870-3872, Aug 1969.

4. Harrison, D.E., Jr., Greiling, D.S., "Computer Studies of Xenon-Ion Ranges in a Finite-Temperature Tungsten Lattice", Journal of Applied Physics, V. 38, No. 8, p 3200-3211, July 1967.

5. Gibson, J.B., Goland, A.N., Milgram, M. and Vineyard, G.H., "Dynamics of Radiation Damage", The Physical Review, V. 120, No. 4, p 1229-1253, Nov 15, 1960.

6. Johnson, R.A., Brown, E., "Point Defects in Copper", The Physical Review, V. 127, No. 2, p 446-454, 15 July, 1962.

7. Erginsoy, C., Vineyard, G.H., and Englert, A., "Dynamics of Radiation Damage in a Body-Centered Cubic Lattice", The Physical Review, V. 133, No. 2A, p A595-A606, 20 Jan 1964.

8. Kornelsen, E.V., Sinka, M.K., "Thermal Release Inert Gases from a (100) Tungsten Surface", Journal of Applied Physics, V. 39, No. 10, p 4546-4555, Sept 1968.

9. Kornelsen, E.V., Sinka, M.K., "Thermal Release Inert Gases from Tungsten; Dependence on the Crystal Face Bombarded", paper presented at Conference on Atomic Collision and Penetration Studies Using Energetic Ions, Chalk River, Sept 1967.

10. Johnson, R.A., "Point Defect Calculations for an fcc Lattice", The Physical Review, V. 145, No. 2, p 423-433, 13 May 1966.

11. Johnson, R.A., Diffusion in Body-Centered Cubic Metals, American Society for Metals, p 357-370, 1965.

12. Girifalco, L.A., Weizer, V.G., "Application of the Morse Potential Function to Cubic Metals", The Physical Review, V. 114, No. 3, p 687-690, 1 May 1959.

13. Girifalco, L.A., Weizer, V.G., "Vacancy Relaxation in Cubic Crystals", Journal of the Physics and Chemistry of Solids, V. 12, p 260-264, 1960.

14. Anderman, A., Computer Investigation of Radiation Damage in Crystals, prepared for Air Force Cambridge Research Laboratories, Office of Aerospace Research, U.S.A.F., Bedford, Mass. 1966.

15. Harrison, D.E., Jr., Gay, W.L., and Effron, H.M., "Algorithm for the Calculation of the Classical Equations of Motion of an N-Body System", Journal of Mathematical Physics, V. 10, No. 7, July 1969.

16. Harrison, D.E., Jr., private communication.

17. Hard, D.W. The Search for a Simple Analytic Representation for a Repulsive Atomic Interaction Potential, M.S. Thesis, Naval Postgraduate School, Monterey, California 1970.

18. Abrahamson, A.A., "Repulsive Interaction Potentials Between Rare-Gas Atoms. Heteronuclear Two-Center Systems", The Physical Review, V. 133, No. 4A, p A990-A1004, 17 Feb 1964.

19. Gay, W.L., Machine Calculations of Energy Transfer Phenomena in a Bombarded Lattice, M.S. Thesis, Naval Postgraduate School, Monterey, California 1963.

20. Levy, N.S., Computer Simulation of the Sputtering Process M.S. Thesis, Naval Postgraduate School, Monterey, California 1965.

21. Johnson, J.P., Calculation of Surface Binding Energies by Computer Simulation of the Sputtering Process, M.S. Thesis, Naval Postgraduate School, Monterey, California 1966.

22. Effron, H.M., Correlation of Argon-Copper Sputtering Mechanisms with Experimental Data Using a Digital Computer Simulation Technique, M.S. Thesis, Naval Postgraduate School, Monterey, California 1967.

23. Moore, W.L., Digital Computer Simulation of Xenon Ions Channeling in the ⟨100⟩ Tungsten Channel at Various Lattice Temperatures, M.S. Thesis, Naval Postgraduate School, Monterey, California 1969.

24. Moore, W.L., unpublished research.

25. Burton, J.J., Jura, G., "Surface Distortion in Face-Centered Cubic Solids", Journal of Physical Chemistry, V. 71, No. 6, May 1967.

26. Harrison, D.E., Jr., Magnuson, G.D., "Sputtering Thresholds", The Physical Review, Vol. 122, No. 5, p 1421-1430, June 1961.

27. Seeger, A., and others, Vacancies and Interstitials in Metals, proceedings of the International Conference on Vacancies and Interstitials in Metals, Julich, Germany, 1968.

INITIAL DISTRIBUTION LIST

		No. Copies
1.	Defense Documentation Center Cameron Station Alexandria, Virginia 22314	2
2.	Library, Code 0212 Naval Postgraduate School Monterey, California 93940	2
3.	Professor D.E. Harrison, Jr., Code 61Hx Department of Physics Naval Postgraduate School Monterey, California 93940	3
4.	Ensign Gary L. Vine Naval Training Center Bainbrige, Maryland 21905	1

Unclassified

Security Classification

DOCUMENT CONTROL DATA - R & D

(Security classification of title, body of abstract and indexing annotation must be entered when the overall report is classified)

1. ORIGINATING ACTIVITY (Corporate author) Naval Postgraduate School Monterey, California 93940	2a. REPORT SECURITY CLASSIFICATION Unclassified 2b. GROUP

3. REPORT TITLE

Computer Simulation of Copper and Tungsten Crystal Dynamics with Vacancies and Interstitials

4. DESCRIPTIVE NOTES (Type of report and, inclusive dates)

Master's Thesis; June 1971

5. AUTHOR(S) (First name, middle initial, last name)

Gary L. Vine

6. REPORT DATE	7a. TOTAL NO. OF PAGES	7b. NO. OF REFS
June 1971	90	27

8a. CONTRACT OR GRANT NO.	9a. ORIGINATOR'S REPORT NUMBER(S)
b. PROJECT NO.	
c.	9b. OTHER REPORT NO(S) (Any other numbers that may be assigned this report)
d.	

10. DISTRIBUTION STATEMENT

Approved for public release; distribution unlimited.

11. SUPPLEMENTARY NOTES	12. SPONSORING MILITARY ACTIVITY
	Naval Postgraduate School Monterey, California 93940

13. ABSTRACT

The effects of point defect implantation in copper and tungsten crystal lattice have been studied by computer simulation techniques. Vacancies, interstitials, and replacement impurities have been created in the first five layers of the free (100) surface of these crystals. The subsequent binding energies of these defects in tungsten were compared with experimental temperature dependent desorbtion peaks, corresponding to binding energies of neon defects in a tungsten crystal. Interstitial and replacement impurity positions in the first three to five layers were found that seem to correspond to the experimental data. Significant results were also obtained which were associated with general surface effects, especially crowdion migration.

DD FORM 1 NOV 65 1473 (PAGE 1)

S/N 0101-807-6811

Unclassified

Security Classification

A-31408

KEY WORDS	LINK A		LINK B		LINK C	
	ROLE	WT	ROLE	WT	ROLE	WT
mputer Simulation						
ngsten Desorbtion Energies						
terstitials in Tungsten						
bstitutional Impurities in Tungsten						

Thesis 128410
V689 Vine
c.1 Computer simulation of copper and tungsten crystal dynamics with vancancies and interstitials.